

PURDUE UNIVERSITY
GRADUATE SCHOOL
Thesis/Dissertation Acceptance

This is to certify that the thesis/dissertation prepared

By Bibin Nataraja Pattel

Entitled

AN EVALUATION OF THE MOVING HORIZON ESTIMATION ALGORITHM FOR ONLINE ESTIMATION OF BATTERY STATE OF CHARGE AND STATE OF HEALTH

For the degree of Master of Science in Mechanical Engineering

Is approved by the final examining committee:

Sohel Anwar

Tamer Wasfy

Lingxi Li

To the best of my knowledge and as understood by the student in the Thesis/Dissertation Agreement, Publication Delay, and Certification/Disclaimer (Graduate School Form 32), this thesis/dissertation adheres to the provisions of Purdue University's "Policy on Integrity in Research" and the use of copyrighted material.

Sohel Anwar

Approved by Major Professor(s): _____

Approved by: Sohel Anwar

12/09/2014

Head of the Department Graduate Program

Date

AN EVALUATION OF THE MOVING HORIZON ESTIMATION ALGORITHM
FOR ONLINE ESTIMATION OF BATTERY STATE OF CHARGE AND STATE
OF HEALTH

A Thesis

Submitted to the Faculty

of

Purdue University

by

Bibin Nataraja Pattel

In Partial Fulfillment of the

Requirements for the Degree

of

Master of Science in Mechanical Engineering

December 2014

Purdue University

Indianapolis, Indiana

This thesis is dedicated to my beloved parents, father C Nataraja Pattel and mother L Usha. All I have and will accomplish are only possible due to your love and sacrifices. I also dedicate this thesis to my lovely wife, Jisha Prakash, who supported me each step of the way; to my beloved brothers, Vinod Nataraja Pattel and Vishnu Nataraja Pattel, who have been instrumental in all my achievements.

ACKNOWLEDGMENTS

I would like to gratefully acknowledge my thesis adviser, Dr. Sohel Anwar for his assistance, guidance, and supervision during the entire course of thesis research and thesis work. Dr. Anwar generously shared with me his research experience and directed me towards perfection in every detail, for which I am always thankful.

I am extremely grateful to my family, colleagues and friends for their support and encouragement.

I would also like to thank my fellow students and colleagues, Vinay K SM, Dr. Nassim Khaled, Dr. Hoseinali Borhan for their help and support during this phase of my life. I thank Ms. Valerie Lim Diemer and Mr. Mark Senn for assisting me in formatting this thesis.

TABLE OF CONTENTS

	Page
LIST OF TABLES	vi
LIST OF FIGURES	vii
ABBREVIATIONS	ix
ABSTRACT	x
1 INTRODUCTION	1
1.1 Overview	1
1.2 Major Contributions of Thesis Work	2
1.3 Organization of this Thesis	3
2 LITERATURE SURVEY	4
2.1 Battery Overview	4
2.2 Battery Applications and Battery Management System	5
2.3 State-of-Charge Estimation Methods	5
2.3.1 Coulomb Counting	6
2.3.2 Voltage Measurement Based Methods	7
2.3.3 Impedance Based Methods	8
2.3.4 Online Estimation Methods	8
2.3.5 Neural Network and Fuzzy Logic Methods	9
2.4 State-of-Health Estimation Methods	9
2.4.1 Monitoring between Cycles	10
2.4.2 Impedance based Methods	10
2.4.3 Computational Modeling for Age Prediction	11
3 EQUIVALENT CIRCUIT BATTERY MODEL AND EXPERIMENTAL VALIDATION	13
3.1 State Variable Description of the Battery Model	14

	Page
3.2 Battery Model Tuning and Validation	18
4 BATTERY STATE ESTIMATION USING EXTENDED KALMAN FILTER AND PROPOSED MOVING HORIZON ESTIMATION	27
4.1 Kalman Filter and Extended Kalman Filter	27
4.2 Implementation of Extended Kalman Filter for the Battery Model	30
4.3 Moving Horizon Estimation	31
4.4 Moving Horizon Estimation Problem Formulation	32
5 COMPARING BATTERY STATE ESTIMATORS EKF AND MHE PERFORMANCES	39
5.1 Estimation Setup and Initialization	39
5.2 Comparing Battery SOC Estimation	40
5.3 Comparing Battery State Estimation	41
5.4 Comparing Root Mean Square Estimation Error	43
5.5 Comparing Battery SOH Estimation	43
6 CONCLUSION	61
6.1 Conclusion	61
6.2 Recommendation for Future Work	62
LIST OF REFERENCES	64

LIST OF TABLES

Table	Page
3.1 Tuned Battery Parameters with Experimental Data	19
5.1 Different Estimator Initial States	39
5.2 Root Mean Square Errors Calculated for Transient Current, SOC Estimation with EKF and MHE	44

LIST OF FIGURES

Figure	Page
3.1 Battery Model Development	14
3.2 RC Battery Equivalent Circuit Model	15
3.3 Battery Model Tuning and Parameter Identification	19
3.4 Battery Model Parameter Identification Using Experimental Tuning Data	20
3.5 Model Bulk and Surface Capacitor Voltages for the Experimental Tuning Data	21
3.6 Battery Model Fit and Parameter Identification Using Experimental Validation Data	22
3.7 Model Bulk and Surface Capacitor Voltages for the Experimental Validation Data	23
3.8 Normalized SOC-OCV Curve LiFePO4 Battery Cell	24
3.9 Battery Model with Scaled Down Drive Cycle Current Data from AUTONOMIE	25
3.10 Model Bulk and Surface Capacitance Voltage for AUTONOMIE Drive Cycle Data	26
4.1 Steps Followed for Battery SOC/SOH Estimation	28
4.2 Kalman Filter Two Step Procedure	29
4.3 Moving Horizon Estimation Concept [37]	33
4.4 Flow Chart for Battery State Estimation	36
4.5 MHE Flow Chart	37
4.6 Matlab Simulink Design for EKF/MHE Estimator and SOC Estimation	38
5.1 Error variability distribution chosen for comparing MHE and EKF performances	40
5.2 SOC Comparison Experimental Data with Low Estimator Initial Condition	41
5.3 SOC Comparison Experimental Data with Same Estimator Initial Condition	42

Figure	Page
5.4 SOC Comparison Experimental Data with High Estimator Initial Condition	43
5.5 SOC Comparison AUTONOMIE Transient Data with Low Estimator Initial Condition	45
5.6 SOC Comparison AUTONOMIE Transient Data with Same Estimator Initial Condition	46
5.7 SOC Comparison AUTONOMIE Transient Data with High Estimator Initial Condition	47
5.8 Battery States Vbulk and Vsurf Estimation Compared for Estimator Initial Condition Case I	48
5.9 Battery States Vbatt and Cbulk Estimation Compared for Estimator Initial Condition Case I	49
5.10 Battery States Vbulk and Vsurf Estimation Compared for Estimator Initial Condition Case II	50
5.11 Battery States Vbatt and Cbulk Estimation Compared for Estimator Initial Condition Case II	51
5.12 Battery States Vbulk and Vsurf Estimation Compared for Estimator Initial Condition Case III	52
5.13 Battery States Vbatt and Cbulk Estimation Compared for Estimator Initial Condition Case III	53
5.14 Comparing the RMS Error for State 1 Vbulk, between the MHE and EKF estimators with various Voltage Sensor Measurement Noise	54
5.15 Comparing the RMS Error for State 2 Vsurf, between the MHE and EKF estimators with various Voltage Sensor Measurement Noise	55
5.16 Comparing the RMS Error for State 3 Vbatt, between the MHE and EKF estimators with various Voltage Sensor Measurement Noise	56
5.17 Comparing the RMS Error for State 4 Bulk Capacitance, between the MHE and EKF estimators with various Voltage Sensor Measurement Noise	57
5.18 Comparing the RMS Error for Estimated SOC, between the MHE and EKF estimators with various Voltage Sensor Measurement Noise	58
5.19 Bulk Capacitance Estimation comparison for SOH Estimation. Healthy and Degraded System I	59
5.20 Bulk Capacitance Estimation comparison for SOH Estimation. Healthy and Degraded System II	60

ABBREVIATIONS

HEV	hybrid electric vehicle
OCV	open circuit voltage
SOC	state of charge
SOH	state of health
SOF	state of function
MHE	moving horizon estimation
KF	Kalman filter
EKF	extended Kalman filter
FL	fuzzy logic
NN	neural network
BMS	battery management system
RMSE	root mean square error

ABSTRACT

Pattel, Bibin Nataraja. M.S.M.E, Purdue University, December 2014. An Evaluation of the Moving Horizon Estimation Algorithm for Online Estimation of Battery State of Charge And State of Health. Major Professor: Sohel Anwar.

Moving Horizon Estimation (MHE) is a powerful estimation technique for tackling the estimation problems of the state of dynamic systems in the presence of constraints, nonlinearities and disturbances and measurement noises. In this work, the Moving Horizon Estimation approach is applied in estimating the State of Charge (SOC) and State of Health (SOH) of a battery and the results are compared against those for the traditional estimation method of Extended Kalman Filter (EKF). The comparison of the results show that MHE provides improvement in performance over EKF in terms of different state initial conditions, convergence time, and process and sensor noise variations. An equivalent circuit battery model is used to capture the dynamics of the battery states, experimental data is used to identify the parameters of the battery model. MHE based state estimation technique is applied to estimates the states of the battery model, subjected to various estimated initial conditions, process and measurement noises and the results are compared against the traditional EKF based estimation method. Both experimental data and simulations are used to evaluate the performance of the MHE. The results shows that MHE performs better than EKF estimation even with unknown initial state of the estimator, MHE converges faster to the actual states, and also MHE is found to be robust to measurement and process noises.

1. INTRODUCTION

1.1 Overview

As per a report of Energy Information Administration the energy consumption all over the world is expected to expand by 50 % by 2030. As the energy requirement needs increase, there is a large requirement for transporting and storing this energy as well. Batteries are the one word solutions for all these energy needs. Batteries power a variety of devices like cell phones and laptops to most sophisticated and tiny devices like pace makers. In the automotive sector batteries plays a major role in the reduction in consumption of fossil oil there by reducing the atmospheric pollution as well. In order to meet the lower energy consumption and emission requirements, electrified vehicles with different modes of electrification including conventional vehicles with start-stop system, hybrid electric vehicles and pure electric vehicles have been developed in the market [1]. In these electrified vehicles, enhanced energy storage systems are utilized to optimize or eliminate the usage of the internal combustion engines. The conventional vehicles with internal combustion engines have a fuel gauge indicator to measure the remaining fuel available at any point of time. But the operation of the electrified vehicles depends also on the battery state as well. Even though hybrid electric vehicles are very common on the road today, packing, managing, monitoring and controlling the battery system in the dynamic automobile environment is still a challenge.

The battery states include state of charge (SOC), state of function (SOF) and state of health (SOH). SOC is a key state of the battery indicates the battery charge capabilities at its current conditions. SOC defines the charge remaining in the battery at any point of time, as a percentage of the stored charge when the battery is fully charged. SOF is estimating the battery functional status. The functional status

depends on the application. For example in start-stop systems where the engine automatically shuts down at vehicle stops, the cranking capability of the battery is the key functional requirements of the battery. SOH is used to monitor the health of the battery for assessing its capacity and power delivering capabilities. SOC and SOH are required to monitor battery functionality (SOF) and to ensure its safe and optimal operation in terms of life and efficiency. Failure to accurately estimate and control SOC can cause under charging or over charging conditions and also can degrade the power and energy delivering capabilities of the battery. So a Battery Management System (BMS) to effectively manage and maintain the battery system in a healthy and long lasting condition is required.

For the effectiveness of the BMS, it needs to know the states (SOC, SOH and SOF) of the battery. Unfortunately none of these key battery parameters are directly measurable with the existing on-board sensing technologies. So a means of estimating the states of the system from the available external measurements which are battery terminal voltage and current is very important. The performance of the estimators varies depending on many factors such as nonlinearities in the system, initial conditions of the estimators and also the measurement system accuracy. In this thesis work A Moving Horizon Estimation technique is applied to estimate the battery SOC and SOH and the performance of the estimator is compared with traditional Extended Kalman Filter.

1.2 Major Contributions of Thesis Work

Main focus of this thesis work is to estimate the SOC and SOH of the battery from the measurable battery current and voltage signals using a Moving Horizon Estimation algorithm. MHE is widely used in Process Control Industry because of its improved performance over the existing estimation technologies such as Kalman and Extended Kalman Filters, but its use was limited in real time on board applications because of the computational complexity it adds. But the computational capability of

the on board computers are increasing day by day which opens the door for complex and more reliable algorithms to be running online. The contributions of this thesis work consists of two parts: First the development of equivalent circuit model of a battery and tune the model's parameters with experimental data using system identification and optimization.

Second using the battery model, implementation of the MHE algorithm to estimate SOC and SOH of the battery and compare the performance with EKF estimator. The performance of the estimators are compared with different estimator initial conditions, and measurement noises. The results and conclusions shows that MHE performs better compared to EKF with a little additional computation cost.

1.3 Organization of this Thesis

This document is organized into four chapters. The history of battery modelling and internal state estimation techniques and application are summarized in Chapter 2. Followed by the development of an equivalent circuit battery model to capture the dynamics and states of the battery cell is explained in Chapter 3. The system identification and tuning of battery model parameters and verification with experimental data is also explained in Chapter 3. The first part of Chapter 4 covers the EKF based estimation technique and latter part covers the proposed MHE based estimation technique. The implementation methodology of both these estimation techniques are explained in detail in this chapter. Chapter 5 compares the performance of these estimation technologies in simulation with different estimator initial conditions and measurement noises. The last chapter concludes the document with the summary of major technical contributions of this work as well as discussion of proposed future work.

2. LITERATURE SURVEY

2.1 Battery Overview

In general batteries fall into two categories. Non rechargeable primary batteries which are commonly found in consumer electronics products. Zinc-carbon, Zinc-Alkaline-MnO₂, Zinc-Air are few examples of primary batteries. Secondary batteries have the capability to recharge. Examples are Lead-Acid, Nickel-Cadmium, Nickel-Metal Hydride and Lithium-Iron batteries. For the hybrid and electric vehicle applications secondary batteries are preferred over primary batteries. The selection of secondary batteries for various vehicular applications depends mainly on their energy density, power density, battery chemistry and their cost [1]. Secondary batteries are made with a series of cells packaged together. A cell is a basic electrochemical unit of the battery. A battery consists of two or more cells assembled in series or parallel configurations to achieve a certain operating voltage/current specification. Since the packaging does not give easy access to internal terminals of each of the cell which are connected together, it is difficult to identify the electrical and chemical status of the individual battery cells from only the available measurements of terminal voltage and current.

An electrochemical cell most likely contains an anode, cathode, electrolyte and a separator [1]. In electrochemical process, an anode is the electrode where the oxidation reaction occurs, where electrons are released to the external circuit. A cathode is the electrode where reduction reaction occurs which collects the electrons emitted from anode through the external circuit with or without a load. For a cell of the battery, during discharge the positive electrode is a cathode and during charge positive electrode is anode, similarly during discharge the negative electrode is an anode and cathode during charge. The electrolyte is the medium that conducts the

ion between the cathode and anode of the cell. The separator is a non-conductive layer that is permeable to ions.

Generally the manufacturer of the battery provides the rated capacity of the battery in the datasheet. The rated capacity is expressed in Ahs (Amp Hrs). The energy density of the battery is normally given in Watt-hours per liter and the power density in Watts per liter [1]. The physical design and construction of the battery heavily influence the performance, energy and power density etc.

2.2 Battery Applications and Battery Management System

A battery management system (BMS) continuously monitors and controls the ability of the battery for certain application. It protects the battery to work within a safe operating region thereby not allowing it to overcharge or over discharge. BMS can also report various other properties of the battery such as maximum charge/discharge current limits, energy delivered, total operating time of the battery, total number of cycles etc. The battery applications can be roughly divided into several categories. Accordingly these applications require the battery monitoring system to provide information such of State of Charge (SOC), State of Health (SOH) and State of Function (SOF). Several techniques are applied in the past to estimate these battery state information, each of them showed certain merits and demerits.

2.3 State-of-Charge Estimation Methods

Theoretically, battery SOC can be determined from terminal measurable quantities including voltage, current and temperature with an appropriate model of the battery; however, model inaccuracies and measurement noises introduce errors in the estimation that become significant over time. Therefore more advanced model-based estimation methods are required to effectively monitor the battery states. In general the SOC can simply be defined by Coulomb counting. SOC can also be described as the charge available for extraction when the terminal voltage is within certain

range and before it reaches a predefined cut-off voltage. The collapse of a battery's terminal voltage is not a good thing for maintaining battery health. Most battery manufacturers provide information on the discharge time vs. terminal voltage for various discharge current rates. A source for potential inconsistency with using only one discharge current vs. terminal voltage curve for SOC to describe the state of the battery is that different discharge current rates will result in differences in the battery energy available for extraction. This phenomenon was first formulated by Peukert's Law [2].

$$KI^{n-1} = Const, n > 1 \quad (2.1)$$

where K is the available battery energy capacity as a function of discharge current I and n is determined by the battery characteristics. When n = 1, the battery is ideal and its capacity is not affected by the discharge current. Typical values for n fall in the range from 1.2 to 1.5. In addition, the battery capacity is also affected by temperature and cut-off voltage limit. The temperature at which the battery operates is directly related to its thermodynamics, which determine the battery OCV. Intuitively, this additional variable will influence the battery discharge capacity defined by a cut-off voltage limit.

2.3.1 Coulomb Counting

A number of techniques have been proposed to measure or monitor the SOC of a battery [3]. The most basic way to estimate SOC is coulomb or charge counting technique. In this method, if the battery capacity as of the total coulombs available Q_{total} when SOC = 1 is known (in normalized per unit), then the current SOC is formulated by

$$SOC = \frac{Q_{total} - \Delta Q_{out}}{Q_{total}} * 100 \quad (2.2)$$

where, ΔQ_{out} is the change of battery charge from a fully charged battery. The coulomb counting SOC estimation method highly depends on the accuracy of the battery and also battery total capacity. The errors in the current measurements and also variations of the battery nominal capacity due to the operating conditions such as ambient temperature and also aging effects lead to accumulated error and SOC drifts from its actual values over time [4] [5]. The coulomb counting SOC estimation method depends highly on the current measurement errors which can cause an accumulated error for coulomb counting that is aggravated over time. If the application allows periodic full recharging, the SOC estimation can be reset in order to overcome this limitation, assuming the recharging algorithm is consistent. The drawbacks of the coulomb counting SOC estimation technique are

1. Correct initial value of the SOC needs to be known.
2. Correct value of the battery capacity needs to be known.
3. Error accumulates over time due to measurement error.
4. Not able recover from wrong SOC values.

2.3.2 Voltage Measurement Based Methods

Battery manufacturers normally specifies the open circuit voltage (OCV) as a function of SOC. So measuring open circuit voltage of the battery is another method for SOC estimation [6]. However it is very difficult to accurately measure a stable open circuit voltage on a continuously working system, a rest time period is required for the battery electrochemical reactions and also diffusion processes to be stabilized. Because of this rest period requirement the opportunities for using this technique to accurately predict SOC in an online battery monitoring application is significantly reduced. Furthermore in real applications, battery is under load and opportunity to measure open circuit voltage is limited. The battery terminal voltage with an external load can be measured online, but it will not indicate the true SOC due to voltage

fluctuations caused by load current variations and the diffusion process dynamics. In addition, battery manufacturers find it difficult to maintain a stable relative terminal voltage even as the battery is being discharged.

2.3.3 Impedance Based Methods

Impedance-based methods are another way to estimate SOC. The basic idea is to measure the impedance spectra for different SOCs and make a correlation of the impedance measurements with the change in SOC. Parameters including high frequency resistance, resonant frequency, and voltage relaxation time constant are being used in this method for correlating with SOC change [7], [8], [9], [10]. A common method in the literature to obtain battery impedance information is impedance spectroscopy. A small excitation signal, normally a sine wave, is injected into the battery and the response is observed to calculate the impedance. In galvanostatic mode, the DC part of the current signal is controlled either at zero or some fixed value, while a small current sine wave is injected. The magnitude of the voltage response needs to be smaller than 10 mV in order to avoid excitation of the nonlinearity of the battery [11]. A complication of this method for measuring battery impedance is that the results can be heavily influenced by the physical wiring connection.

2.3.4 Online Estimation Methods

Various online estimation methods have also been proposed to estimate SOC, i.e., stored energy (not available energy), through schemes such as Kalman filter and impedance parameter estimations. Plett wrote a series of summary papers on the Kalman filter and extended Kalman filter technique for estimating battery internal states, including SOC [12], [13], [14]. To use a Kalman filter to estimate SOC, relationships between SOC and some other measurable quantities, e.g. terminal voltage and current, must first be formulated. Several known relationships between terminal voltage and SOC are used to form a model. Also the long-term diffusion RC time

constant model with a hysteresis phenomenon between the charging and discharging operating regions for the same SOC is another type of model used for estimations. The short-term RC time constant describing the charge exchange is modeled in terms of linearly filtered voltage as a function of the input current that converges to zero when the current is constant. To capture the system parameters offline for the online estimator, least square method can be used for linear models, while an extended Kalman filter can be used for nonlinear models and the parameters are treated as constants with perturbations. Overall, these filter approaches assume the system parameters to be constant and that the process white noise part of the filter equation handles the change of the system parameters over time. Other Kalman filter-based techniques exist in the literature, but the only differences are in how the models are obtained and the assumptions that are made in the process of deriving the models [15], [16], [17], [18].

2.3.5 Neural Network and Fuzzy Logic Methods

There are many other online SOC estimation methods have also been proposed. Neural network [19] and fuzzy logic [20] are few of them. These methods are based on observation laws and system learning. They can be assumed as mathematically advanced Peukert modification methods for dynamic load conditions.

2.4 State-of-Health Estimation Methods

SOH normally is an indicator for battery aging and its capacity to store charge. It has been showed that the aging process comes from the effect of previous battery history [21], [22]. For lithium-ion batteries, it has also been shown that the storage time, storage temperature, and SOC during its storage are related to capacity loss [23]. Additionally, temperature during operation has been identified as a major aging accelerator for batteries due to the facilitation of irreversible reactions [23], [24]. Aging can be detected through a comparison between two discharge cycles. As dis-

cussed above, most battery manufacturers provide discharge time vs. terminal voltage for different discharge current rates. A fresh battery may ideally follow these manufacturer specified curves when discharging while for an aged battery terminal voltage may drop more quickly due to increased internal impedance. If the SOC is evaluated as the total charge available for discharge until the terminal cut-off voltage is reached, then an aged battery will have a lower capacity.

Since the voltage deviation between batteries of different ages can be pronounced for partially-discharged conditions, e.g. SOC = 70 %, it is possible to detect SOH by only partially charging or discharging the battery using the coulomb counting method in order to determine the SOC. This method allows for the detection of major cell failures but is not a reliable method to estimate actual capacity. Several SOH estimation methods based on impedance measurements are also proposed in the literature [25]. Overall two major contributing factors exist to influence the SOH. One is the loss of active material in the battery, causing a loss of capacity. The other is the increase in impedance for various reasons, contributing to an early termination of charging and discharging events.

2.4.1 Monitoring between Cycles

A common method to detect the relative health of a battery is to observe what the capacity is for the same discharge cut-off voltage. This method is commonly used by chemical engineers studying battery aging effects [26], [27]. An obvious prerequisite for this method is to keep the charging and discharging conditions constant, including temperature, current, and cut-off voltages, which makes it impractical for vehicular applications.

2.4.2 Impedance based Methods

For lithium-ion batteries, Blanke et al applied the impedance spectroscopy method to cells subjected to accelerated aging by storing the cells at elevated temperatures.

They report an increase in high-frequency resistance. With the help of the reference node inserted in the tested batteries, both positive and negative electrodes are subjected to impedance spectroscopy. It is found that, while the negative electrode impedance does not change during the accelerated aging test, the positive electrode contributes much of the increase in impedance. The increase in impedance is attributed to the increase in the contact area resistance between the electrical current collector and the positive active mass [27].

Osaka et al conducted a study on lithium-ion batteries aging using impedance spectroscopy. By fitting the results from impedance spectroscopy to their equivalent circuit model, it was determined that the aging process is mainly due to an increase in cathode impedance and anode capacity loss [28].

2.4.3 Computational Modeling for Age Prediction

A summary paper by Sauer et al describes three approaches to predicting aging of a battery during its operating lifetime [29]. The three methods are: physical-chemical processes model, Amp-hour counting model with weighting to emphasize aging during severe operation, and a special event-oriented concept that utilizes pattern recognition to identify severe operating conditions. The physical-chemical processes model has the advantage of being detailed, including many parameters such as SOC, species concentration, etc. The model also self-adjusts to parameters changes due to aging. However, the process of constructing the model, determining the parameters, and computing the model require considerable analysis, experiments, or computational power. The other two methods are less complex and faster in execution, but require expert knowledge to relate the measured data to the aging process.

A simplified moving horizon estimation based state estimation with the cost function involving only the minimization of the error between the model and measurement data and an optimal control of battery management system is described in [30]. In this thesis work the moving horizon estimation cost function takes more terms into the

cost function such as initial conditions in the estimation, process and measurement noise etc.

3. EQUIVALENT CIRCUIT BATTERY MODEL AND EXPERIMENTAL VALIDATION

A dynamic equivalent circuit based model of the battery is presented in this chapter. Equivalent circuit models are widely used for their simplicity and ability to capture all the dynamics of the battery and they are the most favorable model for battery management systems. There are other battery models being used widely such as electrochemical models, but they are very complex models, but are very accurate as they capture each minute behavior and reactions which happens in the battery. So naturally these electrochemical battery models runs very slow. The main focus of this work is to evaluate the feasibility of moving horizon estimation technique for state estimation and this itself is computationally intensive, so to avoid the extra computational overhead of computation an equivalent circuit battery model is considered. There are many variants of the equivalent circuit battery models exists. Most of the models can either estimate only SOC or SOH. The model discussed in this work is chose because employing it enabled to estimate both SOC and SOH with one model.

Figure 3.1 shows the steps followed for battery model development, parameter identification, tuning and validation with experimental data. The model will be discussed in detail and the methodology to populate the model parameters will be shown. The chapter then focuses on the comparison between SOC estimation derived from the model developed and from the coulomb counting method. A generic equivalent circuit model for the battery used in this study is shown in Figure 3.2. The model consists of 3 resistances and 2 capacitors. The bulk capacitor C_{bulk} captures the ability of the battery to store charge, and the capacitor C_{surf} models surface capacitance and diffusion effects. There is a terminal resistance R_{batt} , surface resistance R_{surf} and end resistance R_{end} to model internal resistance of the battery is used as shown in Figure 3.2. The voltage across the bulk and surface capacitors are denoted by V_{bulk}

and V_{surf} respectively [15]. The battery load current I_{batt} is the sum of the branch currents I_{surf} and I_{bulk} . The detailed dynamic state space model development for the equivalent circuit model is described in Section 3.1. For the state space model, 4 states of the system are considered which are $V_{bulk}, V_{surf}, V_{batt}$, and the C_{bulk} . The first three states are important for defining the open circuit voltage behavior of the battery which will be used for the SOC estimation and the fourth state will be used to estimate the aging or capacity of the battery.

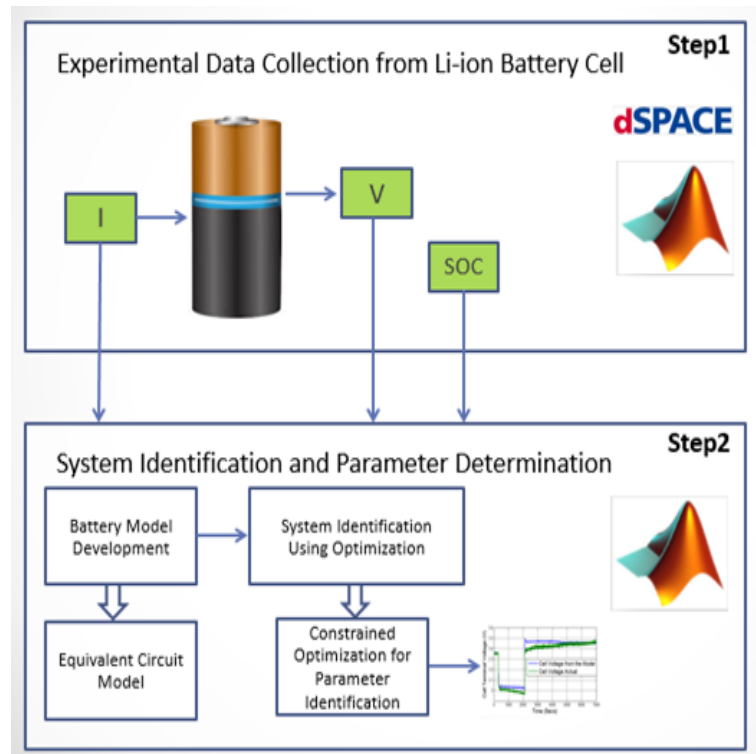


Fig. 3.1. Battery Model Development

3.1 State Variable Description of the Battery Model

In the equivalent circuit model presented in Figure 3.2, the battery terminal voltage can be modeled as

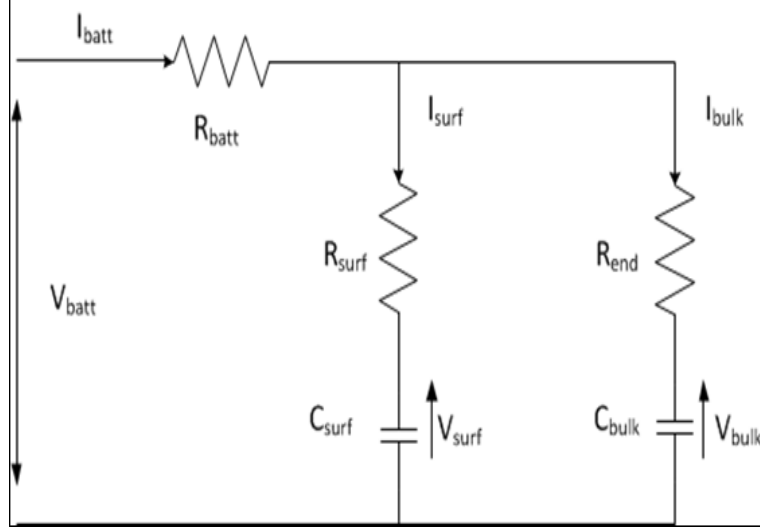


Fig. 3.2. RC Battery Equivalent Circuit Model

$$V_{batt} = I_{batt}R_{batt} + I_{bulk}R_{end} + V_{bulk} \quad (3.1)$$

$$V_{batt} = I_{batt}R_{batt} + I_{surf}R_{surf} + V_{surf} \quad (3.2)$$

By equating Equations 3.1 and 3.2 we get

$$I_{bulk}R_{end} = I_{surf}R_{surf} + V_{surf} - V_{bulk} \quad (3.3)$$

Using Kirchhoffs law, we know that the total current is given by $I_{batt} = I_{bulk} + I_{surf}$

Therefore $I_{surf} = I_{batt} - I_{bulk}$ and substituting in Equation 3.3 and reordering we have

$$\begin{aligned} I_{bulk}R_{end} &= (I_{batt} - I_{bulk})R_{surf} + V_{surf} - V_{bulk} \\ I_{bulk}R_{end} &= I_{batt}R_{surf} - I_{bulk}R_{surf} + V_{surf} - V_{bulk} \\ I_{bulk}R_{end} + I_{bulk}R_{surf} &= I_{batt}R_{surf} + V_{surf} - V_{bulk} \\ I_{bulk}(R_{end} + R_{surf}) &= I_{batt}R_{surf} + V_{surf} - V_{bulk} \end{aligned} \quad (3.4)$$

Assuming that C_{bulk} is a relatively slow varying capacitance and knowing that for a capacitor, current is related to voltage by $I = C \frac{dV}{dt}$, we can assume that

$$I_{bulk} = C_{bulk} \frac{dV_{bulk}}{dt} = \frac{dV_{bulk}}{dt} C_{bulk} (R_{end} + R_{surf}) = I_{batt}R_{surf} + V_{surf} - V_{bulk}$$

$$\frac{dV_{bulk}}{dt} = -\frac{V_{bulk}}{C_{bulk}(R_{end} + R_{surf})} + \frac{V_{surf}}{C_{bulk}(R_{end} + R_{surf})} + \frac{I_{batt}R_{surf}}{C_{bulk}(R_{end} + R_{surf})} \quad (3.5)$$

Similarly $I_{bulk} = I_{batt} - I_{surf}$ and substituting in Equation 3.3 and reordering we get

$$(I_{batt} - I_{surf})R_{end} = I_{surf}R_{surf} + V_{surf} - V_{bulk}$$

$$I_{batt}R_{end} - I_{surf}R_{end} = I_{surf}R_{surf} + V_{surf} - V_{bulk}$$

$$I_{batt}R_{end} + V_{surf} - V_{bulk} = I_{surf}R_{surf} + I_{surf}R_{end}$$

$$I_{batt}R_{end} + V_{surf} - V_{bulk} = I_{surf}(R_{surf} + R_{end})$$

Assuming C_{surf} is also relatively slow varying parameter we have

$$I_{surf} = C_{surf} \frac{dV_{surf}}{dt}$$

$$I_{batt}R_{end} + V_{surf} - V_{bulk} = \frac{dV_{surf}}{dt} C_{surf}(R_{end} + R_{surf}) \quad (3.6)$$

$$\frac{dV_{surf}}{dt} = -\frac{V_{surf}}{C_{surf}(R_{end} + R_{surf})} + \frac{V_{bulk}}{C_{surf}(R_{end} + R_{surf})} + \frac{I_{batt}R_{end}}{C_{surf}(R_{end} + R_{surf})} \quad (3.7)$$

$$\begin{bmatrix} \dot{V}_{bulk} \\ \dot{V}_{surf} \end{bmatrix} = \begin{bmatrix} -\frac{1}{C_{bulk}(R_{end}+R_{surf})} & \frac{1}{C_{bulk}(R_{end}+R_{surf})} \\ \frac{1}{C_{surf}(R_{end}+R_{surf})} & -\frac{1}{C_{surf}(R_{end}+R_{surf})} \end{bmatrix} \begin{bmatrix} V_{bulk} \\ V_{surf} \end{bmatrix} + \begin{bmatrix} \frac{R_{surf}}{C_{bulk}(R_{end}+R_{surf})} \\ \frac{R_{end}}{C_{surf}(R_{end}+R_{surf})} \end{bmatrix} I_{batt} \quad (3.8)$$

Using the voltage divider rule, the output voltage can be written as:

$$V_{batt} = I_{batt}R_{batt} + I_{batt} \frac{R_{end}R_{surf}}{R_{end}+R_{surf}} + V_{bulk} \frac{R_{surf}}{R_{end}+R_{surf}} + V_{surf} \frac{R_{end}}{R_{end}+R_{surf}}$$

Writing in the state equation form, we get

$$V_{batt} = \begin{bmatrix} \frac{R_{surf}}{R_{end}+R_{surf}} & \frac{R_{end}}{R_{end}+R_{surf}} \end{bmatrix} \begin{bmatrix} V_{bulk} \\ V_{surf} \end{bmatrix} + \left[R_{batt} + \frac{R_{end}R_{surf}}{R_{end}+R_{surf}} \right] I_{batt} \quad (3.9)$$

Taking the time derivative of the output voltage and assuming that the battery load current is changing slowly, the rate of change of current over the sampling period is negated and we get:

$$\begin{aligned}
\dot{V}_{batt} = & \left[-\frac{R_{surf}}{C_{bulk}(R_{end}+R_{surf})^2} + \frac{R_{end}}{C_{surf}(R_{end}+R_{surf})^2} \right] V_{bulk} \\
& + \left[\frac{R_{surf}}{C_{bulk}(R_{end}+R_{surf})^2} - \frac{R_{end}}{C_{surf}(R_{end}+R_{surf})^2} \right] V_{surf} \\
& + \left[\frac{R_{surf}^2}{C_{bulk}(R_{end}+R_{surf})^2} + \frac{R_{end}^2}{C_{surf}(R_{end}+R_{surf})^2} \right] I_{batt}
\end{aligned} \tag{3.10}$$

Using the above state equations the open circuit battery voltage is indirectly estimated from the voltage across the bulk and surface capacitances. SOC in this model can be estimated using the voltages across the bulk and surface capacitors based on the relationship between SOC and the open-circuit voltage (OCV). Since C_{bulk} represents the battery bulk-energy capacity, it contributes the majority of the battery SOC as follows [31].

$$SOC = \frac{1}{21} \left[20SOC_{C_{bulk}} + SOC_{C_{surf}} \right] \tag{3.11}$$

Where

$$SOC_{C_{bulk}} = F_{OCV-SOC}(V_{bulk}) \text{ and}$$

$$SOC_{C_{surf}} = F_{OCV-SOC}(V_{surf})$$

Where $F_{OCV-SOC}$ is the function relating open circuit voltage to SOC. It is usually available from battery manufacturers datasheet or experimental data. In this work the OCV-SOC function is developed from experimental data and is used for the SOC estimation.

In order to estimate the bulk capacitance C_{bulk} , an extra state is augmented to the state Equations in 3.8 and 3.10 by

$$\frac{dC_{bulk}}{dt} = 0$$

This assumption is based on the fact that the battery capacity is degraded slowly over time with respect to voltage and SOC dynamics and the rate change in bulk capacitance over the sampling time is very small and negligible. The derivatives of V_{bulk} and V_{batt} are coupled by non-linear elements the battery model now becomes non-linear. The new battery dynamics is summarized by

$$\dot{x} = f(x, u)$$

$$y = C(x)$$

where

$$x = \begin{bmatrix} V_{bulk} \\ V_{surf} \\ V_{batt} \\ \alpha \end{bmatrix}$$

$$f(x, u) = \begin{bmatrix} -\frac{V_{bulk}\alpha}{(R_{end}+R_{surf})} + \frac{V_{surf}\alpha}{(R_{end}+R_{surf})} + \frac{I_{batt}R_{surf}\alpha}{(R_{end}+R_{surf})} \\ \frac{1}{C_{surf}} \left[\frac{V_{bulk}\alpha}{(R_{end}+R_{surf})} + \frac{V_{surf}\alpha}{(R_{end}+R_{surf})} + \frac{I_{batt}R_{end}}{(R_{end}+R_{surf})} \right] \\ V_{bulk} \cdot f1 + V_{batt} \cdot f2 + I_{batt} \cdot f3 \end{bmatrix} \quad (3.12)$$

Where

$$\begin{aligned} f1 &= -\frac{R_{surf}\alpha}{(R_{end}+R_{surf})^2} + \frac{R_{end}}{C_{surf}(R_{end}+R_{surf})^2} - \frac{R_{surf}^2\alpha}{R_{end}(R_{end}+R_{surf})^2} + \frac{R_{surf}}{C_{surf}(R_{end}+R_{surf})^2} \\ f2 &= \frac{R_{surf}\alpha}{R_{end}(R_{end}+R_{surf})} - \frac{1}{C_{surf}(R_{end}+R_{surf})} \\ f3 &= \frac{R_{end}^2}{C_{surf}(R_{end}+R_{surf})^2} - \frac{R_{surf}R_{batt}\alpha}{R_{end}(R_{end}+R_{surf})} + \frac{R_{batt}}{C_{surf}(R_{end}+R_{surf})} + \frac{R_{end}R_{surf}}{C_{surf}(R_{end}+R_{surf})^2} \\ C(x) &= V_{batt} \\ \alpha &= \frac{1}{C_{bulk}} \end{aligned}$$

3.2 Battery Model Tuning and Validation

The battery model is verified with the experimental data taken with 18650 LiFePO4 battery cell. A brock diagram representation of the tuning and validation procedure is shown in Figure 3.3. A current discharge/charge profile as shown in Figure 3.4 is applied to the battery and the battery parameters such as load current, terminal voltage and battery temperature are measured and logged. An optimization algorithm is run in Matlab to fit this experimental cell data on the battery model discussed in Section 3.1. `fmincon` function from the Matlab optimization toolbox is used for this purpose. The cost function selected for optimization is the RMS error between the experimental and model terminal voltage. The optimum value of battery parameters which minimizes the voltage RMSE is given in Table 3.1.

It can be observed from Figure 3.4 that, even though there is a slight difference between the model cell voltage and actual voltage, the basic dynamic behavior is

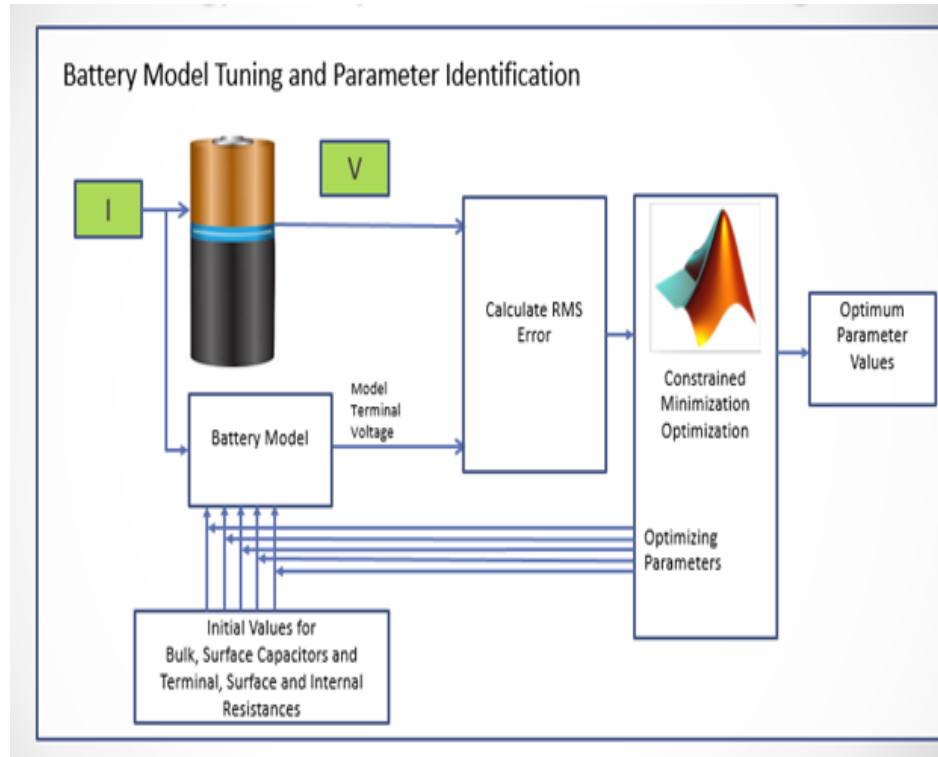


Fig. 3.3. Battery Model Tuning and Parameter Identification

Table 3.1
Tuned Battery Parameters with Experimental Data

Parameter	Optimum Value for Experimental Data	Units
R_{end}	0.019090364750000	Ohms
R_{surf}	0.020667571400000	Ohms
R_{batt}	0.237528699690000	Ohms
C_{bulk}	88370.8300398	Farads
C_{surf}	81.99975609	Farads

captured. The difference may be because of the changes in initial condition estimates of the model. Figure 3.5 shows the bulk and surface capacitance voltages from the model for the experimental data. The model and the identified parameters are validated on a different experimental data set and the validation results are shown in

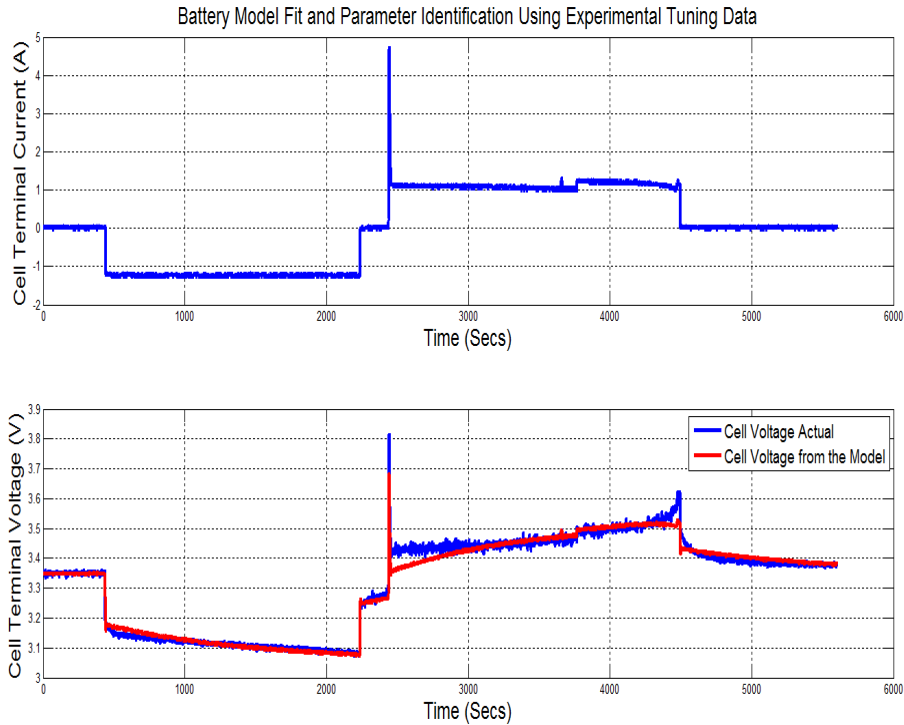


Fig. 3.4. Battery Model Parameter Identification Using Experimental Tuning Data

Figure 3.6 and Figure 3.7. The relationship between the open circuit voltage and SOC is also found experimentally. The SOC-OCV trend for the battery cell under experiment is shown in Figure 3.8.

The battery model is tuned and validated on different data sets as shown in above Figures. After the tuning and validation the model is ran with a transient battery current signal from a passenger Hybrid car model of the AUTONOMIE [32] software (developed by Argonne National Laboratory) to evaluate the performance on a real world charge discharge profile. The selected transient current signal is scaled down appropriately for evaluating the transient performance of the battery model developed. The scaled down transient current signal is shown in Figure 3.9. This current input signal is used for all the validation of the state estimator performances for this work. Figure 3.10 shows the modeled bulk and surface capacitance for the transient current data.

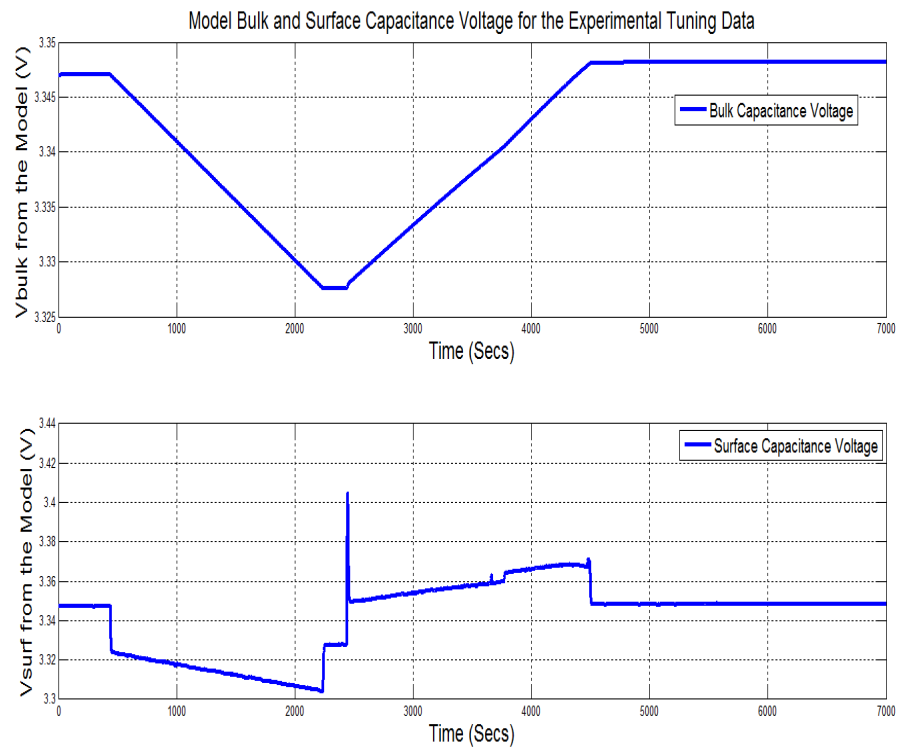


Fig. 3.5. Model Bulk and Surface Capacitor Voltages for the Experimental Tuning Data

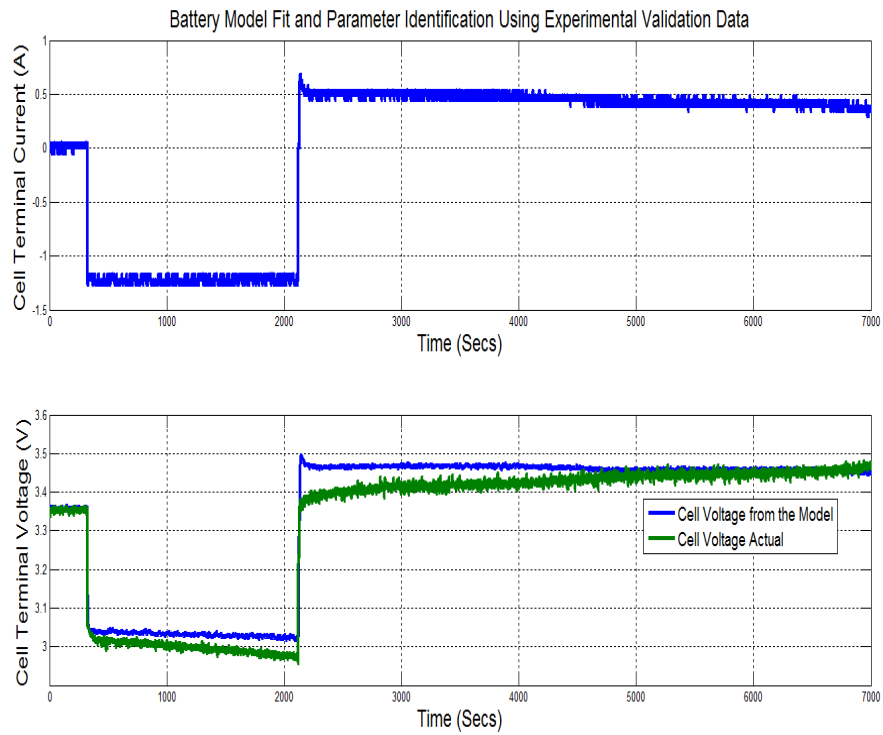


Fig. 3.6. Battery Model Fit and Parameter Identification Using Experimental Validation Data

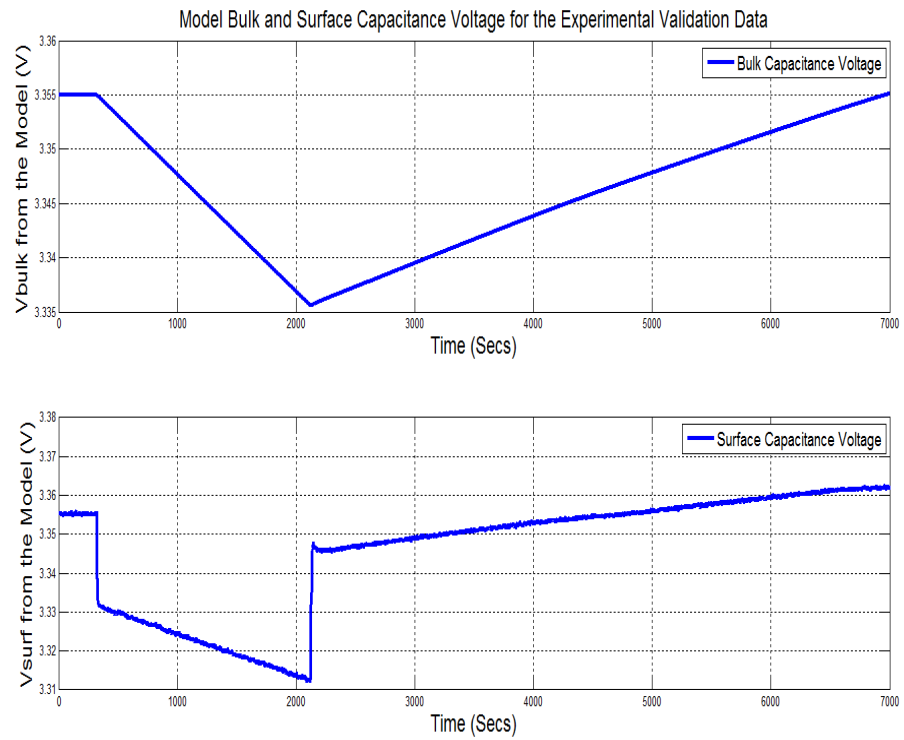


Fig. 3.7. Model Bulk and Surface Capacitor Voltages for the Experimental Validation Data

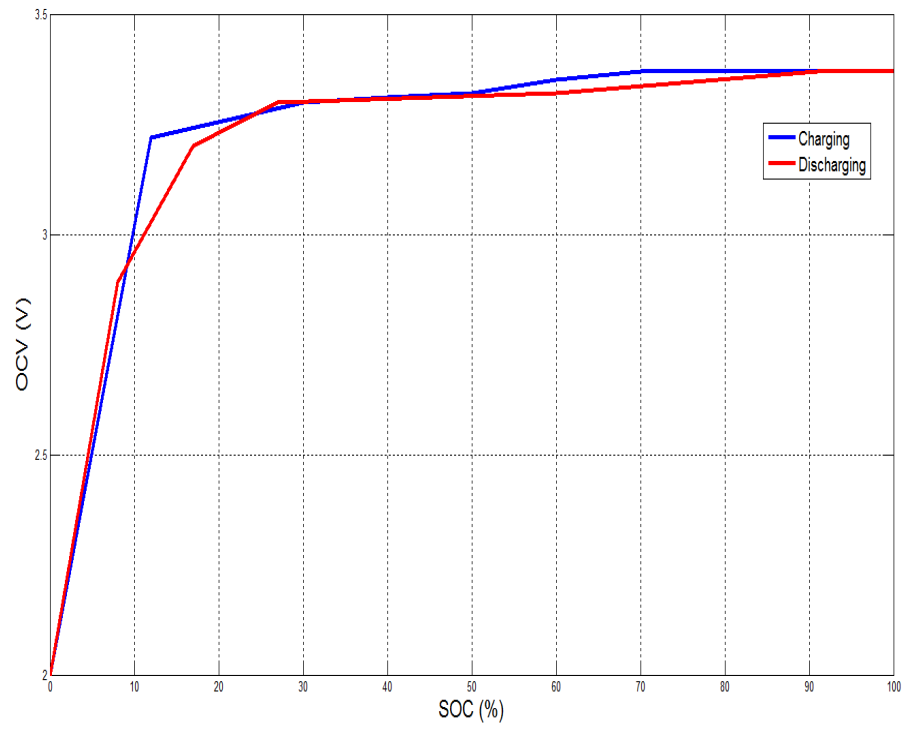


Fig. 3.8. Normalized SOC-OCV Curve LiFePO4 Battery Cell

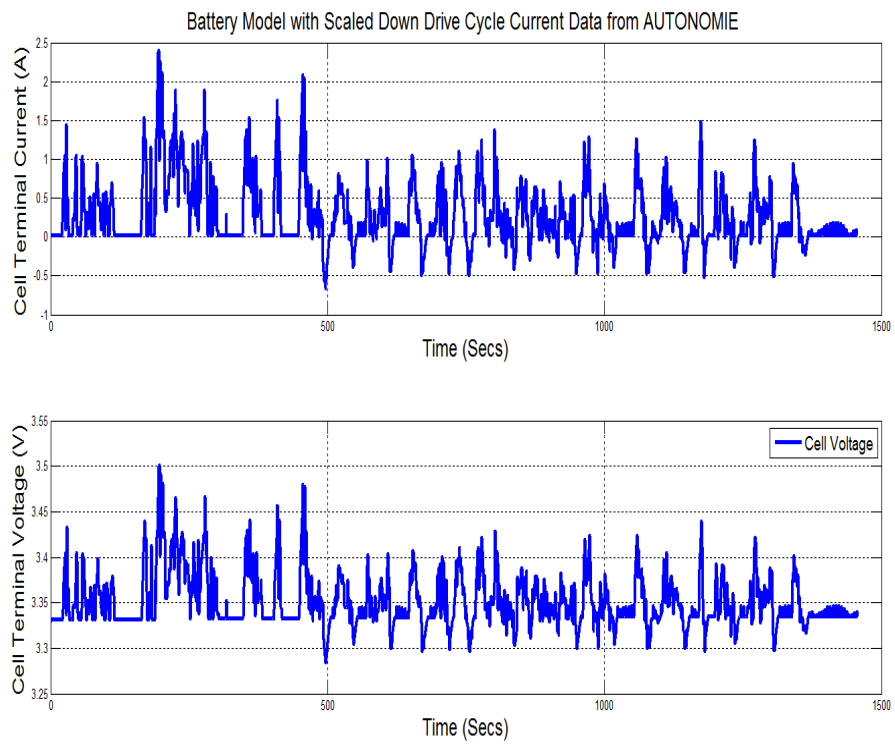


Fig. 3.9. Battery Model with Scaled Down Drive Cycle Current Data from AUTONOMIE

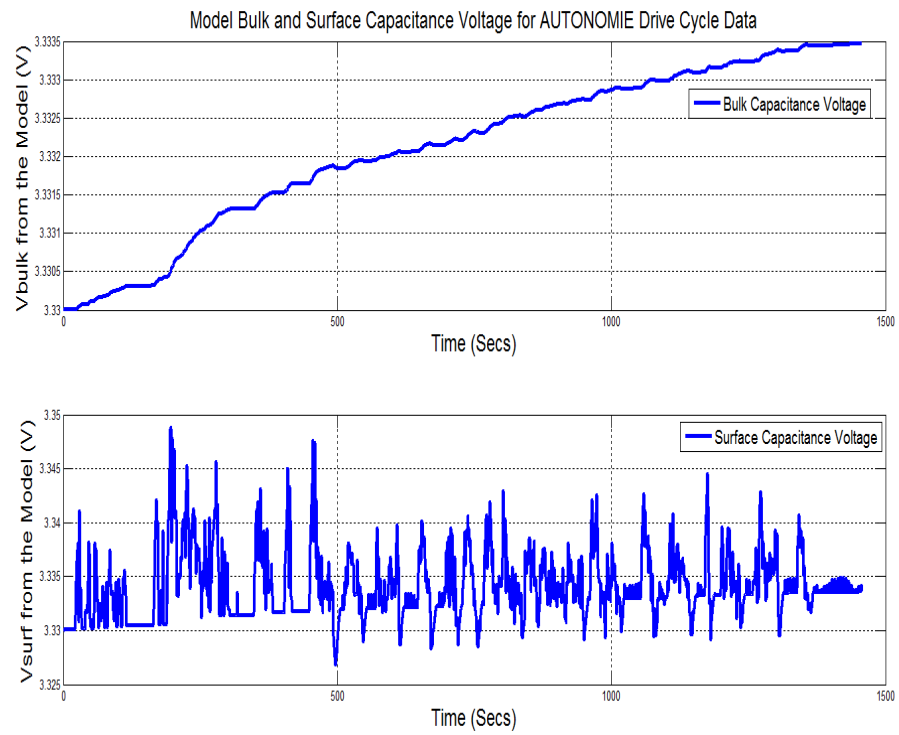


Fig. 3.10. Model Bulk and Surface Capacitance Voltage for AUTONOMIE Drive Cycle Data

4. BATTERY STATE ESTIMATION USING EXTENDED KALMAN FILTER AND PROPOSED MOVING HORIZON ESTIMATION

The first part of this chapter describes in detail the traditional Kalman and Extended Kalman Filters (EKF) for state estimation of dynamic systems under measurement noises and nonlinearities. The second part talks about the proposed Moving Horizon Estimation (MHE) for the battery state estimation. Simulation study is carried out for comparing the performances of MHE and EKF. Figure 4.1 shows the steps followed for the parameter estimation. Process and measurement noise is introduced into the estimator as shown and the robustness of the estimator to these variations is analyzed. Both EKF and MHE estimators are ran parallelly to estimate the states of the battery model and these states are used for estimating the SOC and SOH. A comparison is made between the EKF and MHE estimated SOC and SOH with the actual known values.

4.1 Kalman Filter and Extended Kalman Filter

The Kalman filter (KF) is a standard method for unconstrained state estimation for a linear system and is a common benchmark for comparison with other estimators. Extended Kalman filter applies the same Kalman Filter technique on the non-linear systems except that the nonlinear system is first linearized at every operating point. This section gives a brief overview of the Kalman filter and more details can be found in the related literature. The Kalman Filter implements a two-step process to calculate the a-posteriori Bayesian estimate [33]. The first step is the time update and second step is the measurement update. In the first step the system model is used to predict the current state of the system based on the previous estimate. The estimator

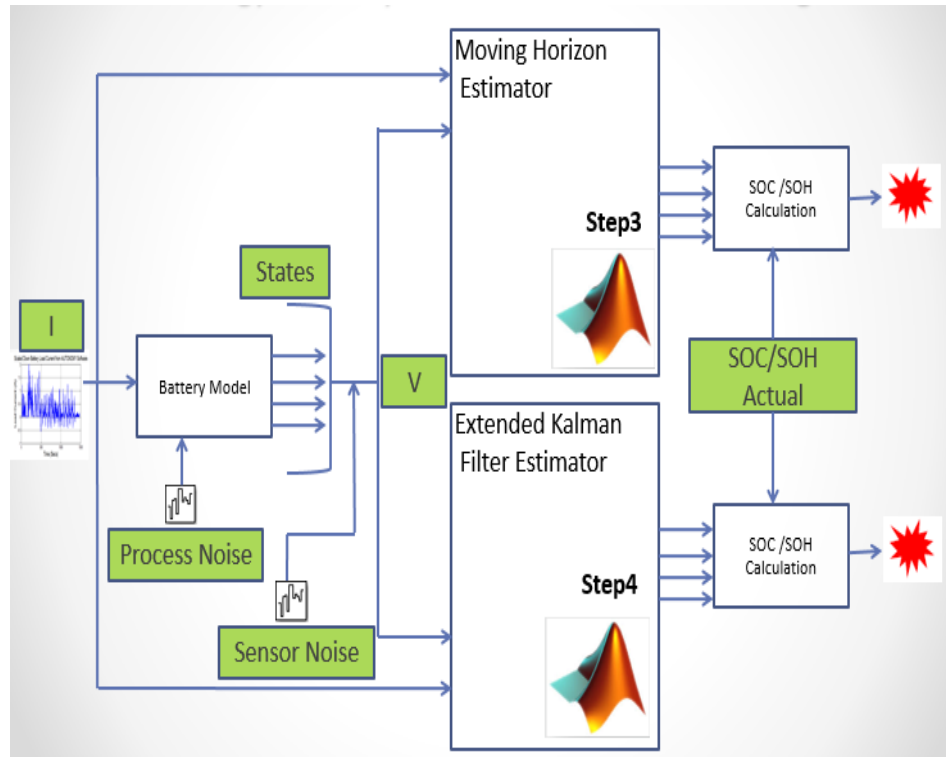


Fig. 4.1. Steps Followed for Battery SOC/SOH Estimation

has to be initialized with a reasonable initial condition for the algorithm to start. In the second step the prediction from first step is updated using the sensor information. So Kalman filter is a prediction-correction based estimator which minimizes the error covariance between model and sensor.

The Kalman filter uses a series of measurements gathered over time, which contains noises and other inaccuracies, and produces estimates of unknown state variables. In other words, the Kalman filter operates recursively on noisy input data to produce a statistically optimal estimate of the underlying system state. For a nonlinear system mentioned in Chapter 3, an extended Kalman Filter is required where the nonlinear model is linearized in each time step.

In Figure 4.2 A_d is the system matrix, B_d the input matrix, C_d the output matrix $x_{k+1|k}$ is the predicted state and $x_{k+1|k+1}$ is the corrected state. Q and R represents the measure of confidence in the model and the measurement. The larger the entries

in R are in relation to Q the more relative trust is put into the measurements over the system model. P is the covariance matrix and K is the Kalman Filter gain.

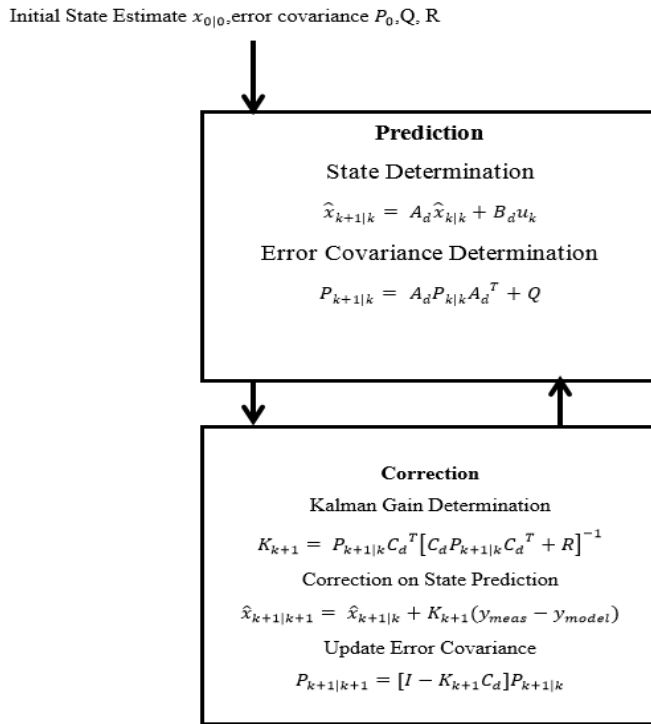


Fig. 4.2. Kalman Filter Two Step Procedure

The Kalman filter is a state estimator which is optimum for a linear dynamic systems. Though KF is originally developed and proved for linear systems estimation of non-linear systems can also be performed using some modifications to the original KF. An Extended Kalman Filter (EKF) is a modified version of KF which is popularly used for the estimation of non-linear systems. The EKF linearizes the non-linear model around an operating point and apply the normal KF technique for the state estimation. But EKF is observed to be very sensitive to estimator initialization. The filter can diverge and go unstable very easily because of wrong initial estimation and if the noise matrices are not chosen appropriately [34].

4.2 Implementation of Extended Kalman Filter for the Battery Model

Figure 4.2 shows the discrete time recursive Kalman Filter algorithm [15]. To implement EKF, the state Equations 3.12 are linearized around the current operating conditions as

$$\delta \dot{x} = F(x)\delta x + B\delta u, \delta y = C\delta x \quad (4.1)$$

Where in Equation 4.1 we have

$$\delta x = x - x_0, \delta u = u - u_0$$

$$F(x) = \frac{\partial f}{\partial x} = \begin{bmatrix} F(1,1) & F(1,2) & F(1,3) & F(1,4) \\ F(2,1) & F(2,2) & F(2,3) & F(2,4) \\ F(3,1) & F(3,2) & F(3,3) & F(3,4) \\ F(4,1) & F(4,2) & F(4,3) & F(4,4) \end{bmatrix}$$

$$F(1,1) = -\frac{\alpha}{(R_{end}+R_{surf})}$$

$$F(1,2) = \frac{\alpha}{(R_{end}+R_{surf})}$$

$$F(1,3) = 0$$

$$F(1,4) = -\frac{V_{bulk}}{(R_{end}+R_{surf})} + \frac{V_{surf}}{(R_{end}+R_{surf})} + \frac{I_{batt}R_{surf}}{(R_{end}+R_{surf})}$$

$$F(2,1) = \frac{1}{C_{surf}(R_{end}+R_{surf})}$$

$$F(2,2) = -\frac{1}{C_{surf}(R_{end}+R_{surf})}$$

$$F(2,3) = 0$$

$$F(2,4) = 0$$

$$F(3,1) = -\frac{R_{surf}\alpha}{(R_{end}+R_{surf})^2} + \frac{R_{end}}{C_{surf}(R_{end}+R_{surf})^2} - \frac{R_{surf}^2\alpha}{R_{end}(R_{end}+R_{surf})^2} + \frac{R_s}{C_{surf}(R_{end}+R_{surf})^2}$$

$$F(3,2) = 0$$

$$F(3,3) = \frac{R_{surf}\alpha}{R_{end}(R_{end}+R_{surf})} - \frac{1}{C_{surf}(R_{end}+R_{surf})}$$

$$F(3,4) = \frac{V_{bulk}R_{surf}}{(R_{end}+R_{surf})^2} - \frac{V_{bulk}R_{surf}^2}{R_{end}(R_{end}+R_{surf})} + \frac{V_{batt}R_{surf}}{R_{end}(R_{end}+R_{surf})} - \frac{I_{batt}R_{surf}R_{batt}}{R_{end}(R_{end}+R_{surf})}$$

$$F(4,1) = 0$$

$$F(4,2) = 0$$

$$F(4,3) = 0$$

$$F(4,4) = 0$$

$$B = \frac{\partial f}{\partial u} = \begin{bmatrix} \frac{R_{surf}\alpha}{(R_{end}+R_{surf})} \\ \frac{R_{end}}{C_{surf}(R_{end}+R_{surf})} \\ f3 \\ 0 \end{bmatrix}$$

$$C = \begin{bmatrix} 0 & 0 & 1 & 0 \end{bmatrix}$$

For applying the discrete time EKF equations and MHE on the battery model discussed above, the continues time model is discretized in the implementation.

$$\delta\dot{x} = A_k\delta x + B_k\delta u, \delta y = C\delta x$$

Where $A_k = F(x)|_{x_k}, u_k$ can be discretized to give

$$x_{k+1} = A_d x_k + B_d u_k$$

$$y_{k+1} = C_d x_{k+1}$$

Where $A_d = I + \frac{\partial f}{\partial x}$

$$B_d = B T_c$$

$$C_d = C$$

4.3 Moving Horizon Estimation

Moving Horizon Estimation (MHE) is a powerful estimation technique that has obtained attention in connection with the increased application of model predictive control [35]. A model predictive controller controls a system by solving an open-loop optimal control problem in which the current states of the plant is used as the initial states. Predictive controllers are said to be the dual of MHE, which estimates the state variables by using a moving window of most recent information and carry over the last estimate to the next time instant. MHE is an optimization based estimation approach that uses a series of continuously sampled measurements over time, which contains noise and other inaccuracies and estimates of unknown variables or states of the system. In MHE the system state and disturbances are estimated by solving a constrained optimization problem. So the knowledge about the system can be added as constraints, to improve the optimization results. The constraints may be

representing system behavior such as non-negativity of battery terminal voltage, or non-zero mean noise of sensor measurement variability, and these known constraints can significantly improve the performance of estimator.

The interest in MHE was originally generated because of its robustness in the presence of modelling and sensing uncertainties and numerical errors. In this thesis work, a MHE for the battery state estimation is implemented. The proposed MHE technique minimizes a quadratic estimation cost function defined on a moving window. The moving window contains a series of measurement data, disturbances, model outputs and initial conditions. Whereas the Kalman filter considers only one set of measurements at a time. In it is shown that the Kalman filter is the algebraic solution to an unconstrained least square optimization problem. It is shown that MHE reduces to the Kalman filter with simplified conditions [36]. There are several evaluations of the extended Kalman filter and MHE carried out on linear and non-linear systems, results showed MHE showed improved performance over EKF with some added computational cost [36]. Because of this added computational expense, MHE so far has only been applied to systems with greater computational power such as process industries. However today's vehicle on-board computers and other battery management devices are becoming more and more computational capable and online optimization based estimation and control approaches are becoming more practical to improve the system performance over the traditional approaches.

4.4 Moving Horizon Estimation Problem Formulation

With a given state space model and series of measurements in a window of size N starting from time $k - N + 1$ up to k , all the states in this moving window can be estimated by solving a minimization problem [36]. Figure 4.3 shows the concept of Moving Horizon Estimation. The estimator algorithm continuously tries to minimize the error between the estimated and actual output in a moving window consisting of certain number of samples.

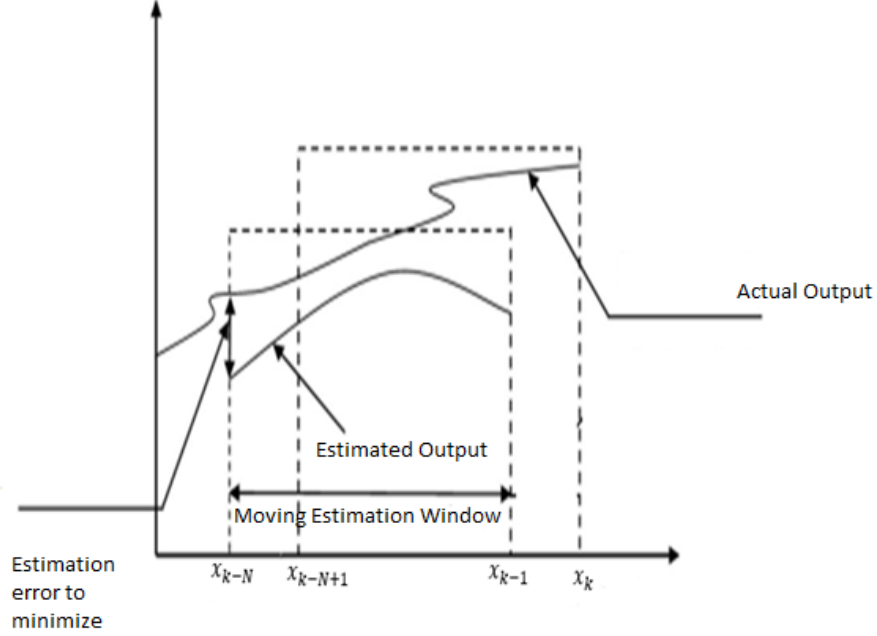


Fig. 4.3. Moving Horizon Estimation Concept [37]

$$\min_{x_{k-N+1} \dots x_k} \left[\begin{aligned} & (x_{k-N+1}^e)^T P_{k-N+1|k-N}^{-1} x_{k-N+1}^e + \sum_{l=k-N+1}^k v_l^T R^{-1} v_l \\ & + \sum_{l=k-N+1}^{k-1} w_l^T Q^{-1} w_l \end{aligned} \right] \quad (4.2)$$

where

$$x_{k-N+1}^e = x_{k-N+1} - x_{k-N+1|k-N}$$

$$v_l = y_l - g(x_l)$$

$$w_l = x_{l+1} - f(x_l)$$

k is the current sample time.

l is the loop index for the optimization cost function.

This optimization problem now opens the possibility to add system knowledge in the form of constraints. The constraints might for example capture the fact that a battery terminal voltage will always be positive or account for non-zero non-Gaussian noise [38]. So the above optimization problem is not equivalent to Kalman Filter any-

more where it only used the measurement of the current time step and a covariance update term to predict the next state. One way to improve the estimator performance is to use more samples of past measured data. But if we use all the past available measurement information for the constrained estimation Equation 4.2, then the estimation problem grows unboundedly with time. This is called as Full Information Estimator [39]. A Full Information Estimator leads to very high computational cost as the estimator needs to process all the previous time step dataset from the start of the estimation for the estimation algorithm. In order to keep the estimation problem computationally efficient it is necessary to limit the data used for estimation for every time step, for example by discarding the oldest measurement once a new one becomes available. This essentially slides a window over the data, leading to the moving horizon estimator (MHE). The old time step data that is not considered any more can be accounted for by the so called arrival cost so that the information is not lost. The MHE then considers only a limited amount of data.

There are three major terms in the above objective function. The first term x_{k-N+1}^e consists of the error between the initial state in the moving horizon, x_{k-N+1} , (this initial state is varied in the optimization process), and a priori state estimate $x_{k-N+1|k-N}$ at the beginning of the horizon. So for the very first execution of the MHE $x_{k-N+1|k-N}$ will be the estimator's initial state guessed by the user based on system knowledge and past behavior of the system. In general the estimate $x_{k|i}$ is defined as the state estimate at time k given measurements up to time i . The term $x_{k-N+1|k-N}$ denotes a priori estimate at time $k-N+1$ based on the data up to $k-N$. $P_{k-N+1|k-N}$ is the covariance of the state estimation error in the a priori estimate. Covariance term is updated at every step after the correction is applied to the priori estimate. The inverse of $P_{k-N+1|k-N}$ is used as a weighing matrix for x_{k-N+1}^e in the objective function.

The second term $v_l = y_l - g(x_l)$ is the error between the measurement and sensor model prediction. Here y_l indicates the measurement data collected over the moving window. All the measurement data from time $k-N+1$ up to k is collected and the

error is calculated with the corresponding model data and the optimization algorithm tries to estimate the initial state of the system which will minimize this error. R is the covariance matrix of the sensor model uncertainty. The inverse of R is used as a weighing matrix for v_l in the objective function. Similarly the final term $w_l = x_{(l+1)} - f(x_l)$ is the error between the estimated state and its process model. Q is the covariance of the process model uncertainty w . The inverse of Q is used as the weighing matrix for w in the objective function.

MHE can consider only a limited amount of past data in order to be computationally feasible. It discards the old data set as the new information becomes available, but the discarded data is simply not thrown away, instead it is preserved through an arrival cost [39]. The arrival cost update needs to be updated at every time step and should be done carefully because a wrongly chosen arrival cost can drive the estimator to become unstable. The minimization problem estimates the optimal states inside a moving window consisting of the most recent N measurements. The window starts at time $k - N + 1$ and spans up to k . The MHE moves the window in order to include the new data when the new measurements are available and discards the old data. When the window shifts, the initial state in the window $x_{(k-N+2|k-N+1)}$ must be updated so that the information from the previous window can be carried to the new window. A common scheme for updating the MHE is to use the extended Kalman filter [36]. The correction and update equations used for MHE are:

$$L_{k-N+1} = P_{k-N+1|k-N} C_{k-N+1|k}^T * (C_{k-N+1|k} P_{k-N+1|k-N} C_{k-N+1|k}^T + R)^{-1} \quad (4.3)$$

$$x_{k-N+1|k-N+1} = x_{k-N+1|k-N} + L_{k-N+1} * (y_{k-N+1} - g(x_{k-N+1|k})) \quad (4.4)$$

$$P_{k-N+1|k-N+1} = (I - L_{k-N+1} C_{k-N+1|k}) P_{k-N+1|k-N} \quad (4.5)$$

The measurement prediction terms of EKF for MHE are:

$$x_{k-N+2|k-N+1} = f(x_{k-N+1|k}) + A_{k-N+2|k} (x_{k-N+1|k-N+1} - x_{k-N+1|k}) \quad (4.6)$$

Where $C_{k-N+1|k} = \frac{\partial g(x)}{\partial x|x=x_{k-N+1|k}}$ and $A_{k-N+1|k} = \frac{\partial f(x)}{\partial x|x=x_{k-N+1|k}}$

In order to ensure a good estimate of the system the stability of the MHE plays a major role. The stability conditions of MHE are discussed in [39] for a nominal system with no process and measurement noises. Figure 4.4 the flow chart of the estimation and Figure 4.5 shows the flow chart specific to MHE. Figure 4.6 shows the Matlab Simulink block diagram logic developed for the EKF and MHE estimators.

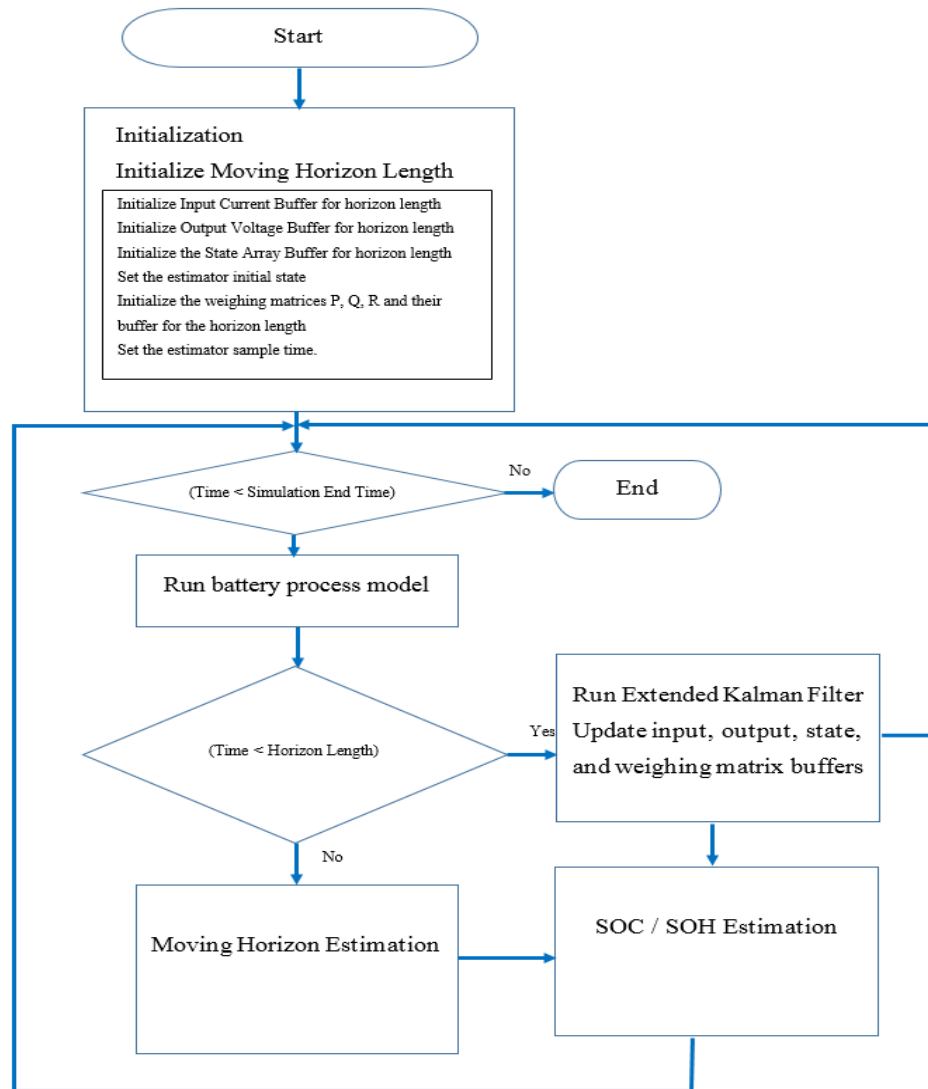


Fig. 4.4. Flow Chart for Battery State Estimation

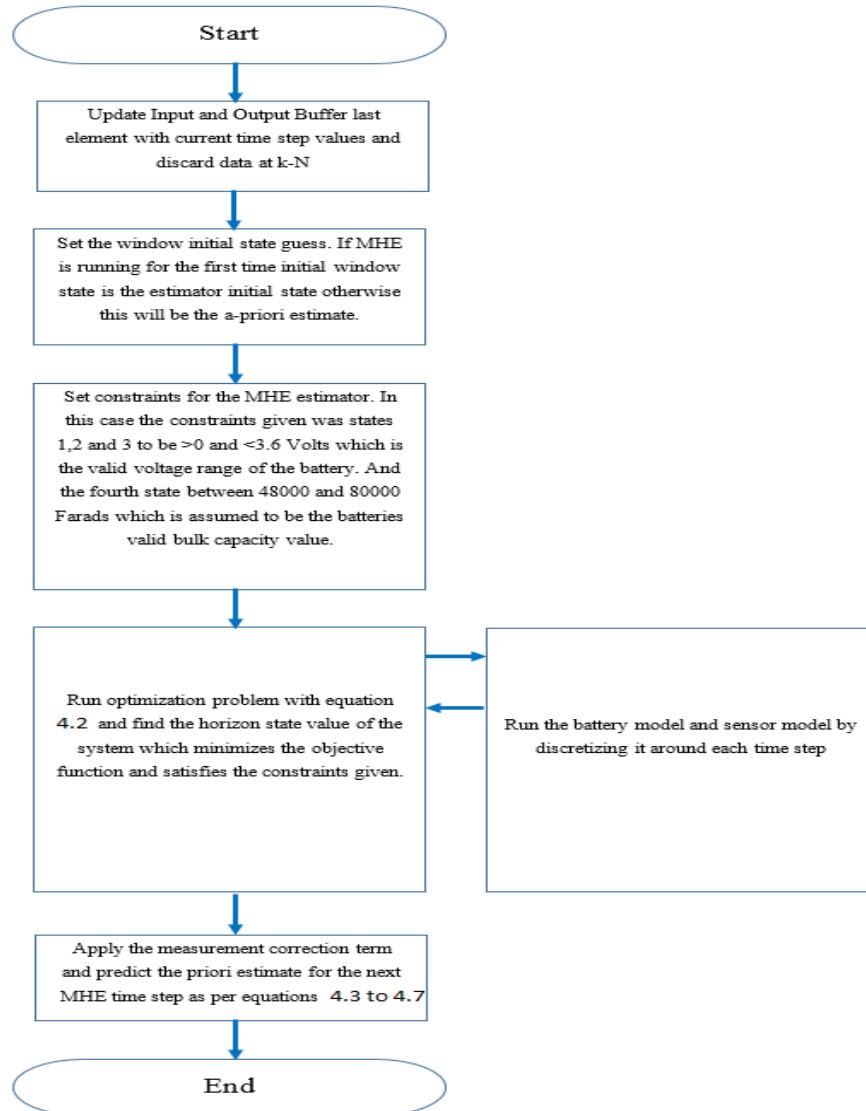


Fig. 4.5. MHE Flow Chart

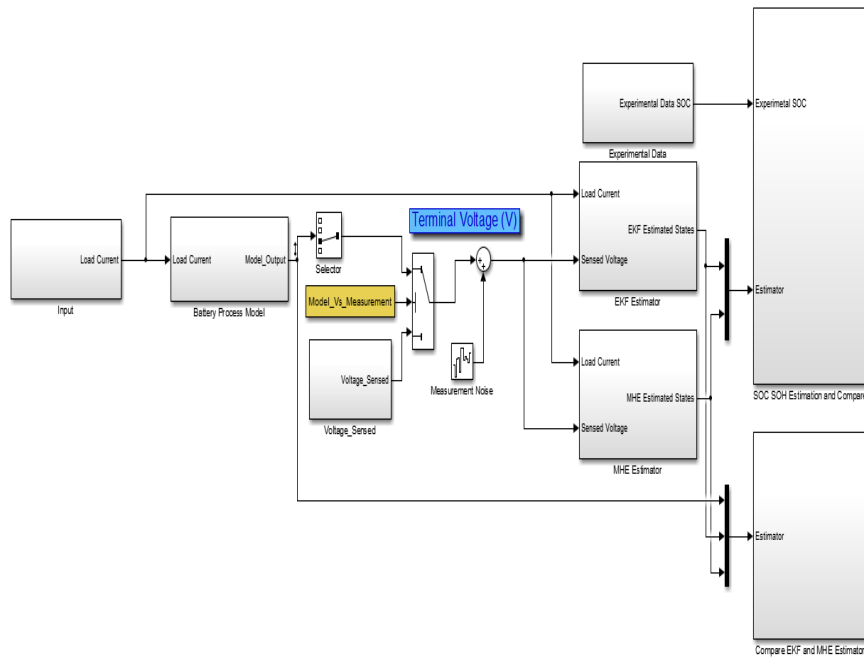


Fig. 4.6. Matlab Simulink Design for EKF/MHE Estimator and SOC Estimation

5. COMPARING BATTERY STATE ESTIMATORS EKF AND MHE PERFORMANCES

5.1 Estimation Setup and Initialization

In this chapter the performance of EKF and MHE estimators for the battery SOC and SOH estimations are compared. The estimator performances are compared for the experimental data used for battery model identification and also on a transient battery current signal from a passenger hybrid car model of the AUTONOMIE software (developed by Argonne National Laboratory). The battery current signal from the AUTONOMIE is selected and scaled it down appropriately for evaluating the battery model and estimation techniques as shown in 3.9. EKF and MHE simulations are ran with a measurement noise of $+/- 0, 0.5, 12, 5, 10, 20, 30,$ and 40% variabilities added to the output voltage and also with different estimator initial conditions. The error distribution of the output voltage used for the simulations is shown in Figure 5.1 and the three different initial conditions used for the estimators are shown in Table 5.1. A horizon length of 5 samples is used for the MHE simulations.

Table 5.1
Different Estimator Initial States

	Case I	Case II	Case III
Est Init State	[0 0 0 0]	[3.35 3.35 3.35 0.88]	[6.71 6.71 6.71 1.76]
Act Init State	[3.35 3.35 3.35 0.88]	[3.35 3.35 3.35 0.88]	[3.35 3.35 3.35 0.88]

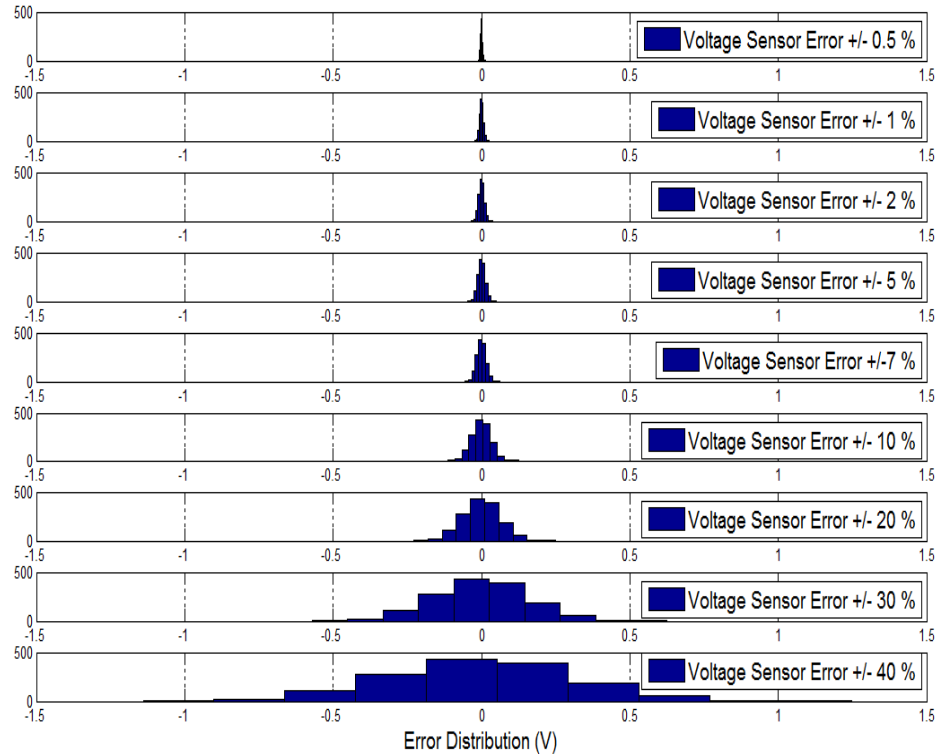


Fig. 5.1. Error variability distribution chosen for comparing MHE and EKF performances

5.2 Comparing Battery SOC Estimation

Simulation results show that in all these cases MHE performs better than EKF in terms of estimation capabilities including faster convergence irrespective of the estimator initial conditions and robust estimation against different sensor variations. However, due to additional computational cost, for each time step MHE ran about 1.5 times slower compared to EKF. Both EKF and MHE are implemented with a sample time of 1 second. All the simulations are ran on a 64 bit Windows 8 machine.

Figures 5.2, 5.3, 5.4 shows the Actual, EKF estimated and MHE estimated SOC for the experimental data and Figures 5.5, 5.6, 5.7 shows the SOC for the AU-TOONOMIE transient current input. Battery SOC is calculated from the estimated voltages V_{bulk} (state 1) and V_{surf} (state 2) from both MHE and EKF and the OCV-SOC curve shown in Figure 3.8. The SOC estimated from MHE signals shows better

match with the actual SOC compared to EKF under different estimator initial conditions. The results shows some discrepancies in the estimator vs actual SOC. This is because the estimator SOC calculation is based on the estimated open circuit voltage for the battery model, whereas in AUTONOMIE SOC was calculated using coulomb counting method which gives a smoother signal. But it can be noted that using the OCV based estimation the initial SOC condition at the start of the simulation is not important. MHE shows better convergence to the actual SOC in all these plots.

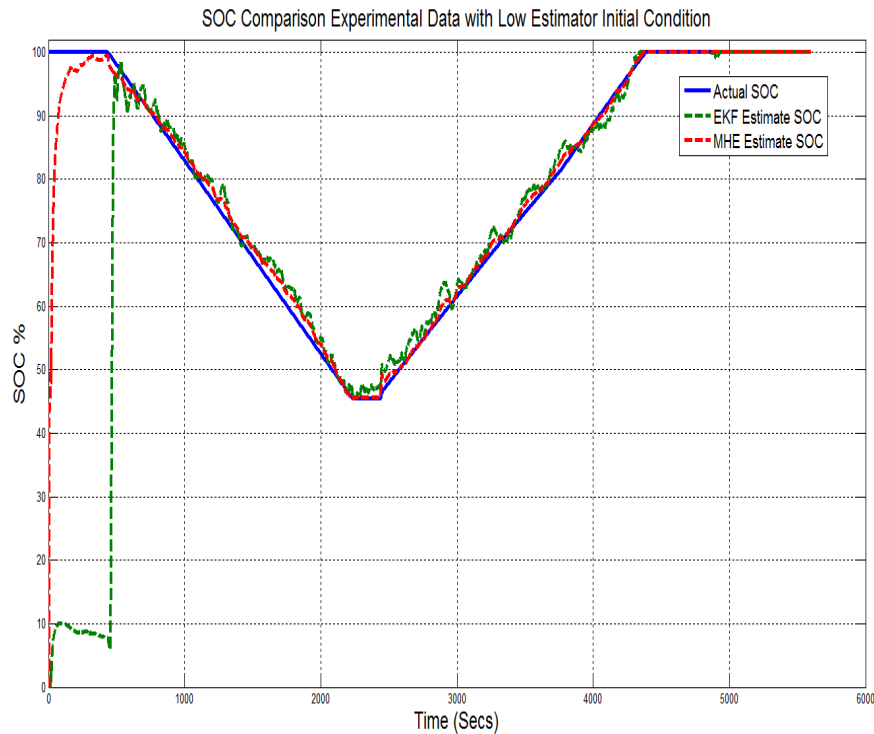


Fig. 5.2. SOC Comparison Experimental Data with Low Estimator Initial Condition

5.3 Comparing Battery State Estimation

Figures 5.8, 5.9, 5.10, 5.11, 5.12, 5.13 (pages 48 - 53) shows the EKF and MHE estimator performances with different estimator initial conditions for all 4 states of the battery model. The percentage estimation error with respect to the actual values

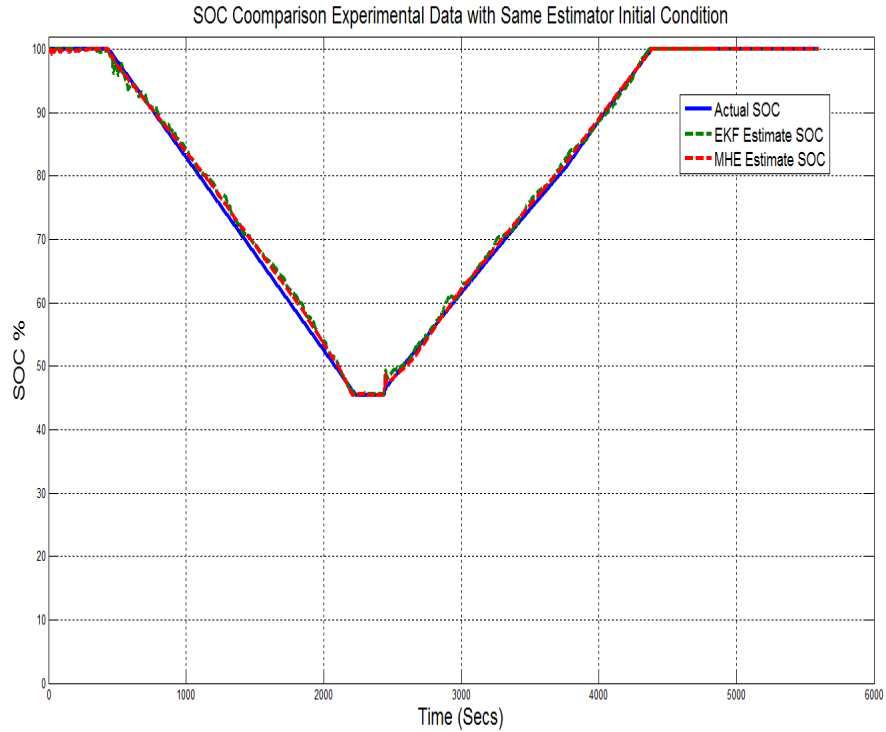


Fig. 5.3. SOC Comparison Experimental Data with Same Estimator Initial Condition

are also shown in these Figures. It can be seen that even though the estimators are initialized to different initial conditions (far off from the actual values) MHE converges to the actual states very quickly compared to the EKF. The convergence time for the states for EKF is observed to be about 100 Secs compared to about 10 Secs for MHE. In Case I and Case III EKF could not converge to the actual value for the state 4 which is a measure of bulk capacitance as shown in Figure 5.8 and 5.13. Figures 5.14, 5.15, 5.16, 5.17, 5.18 (pages 54 - 58) shows the RMS errors calculated for the estimators for different sensor error variations mentioned above and it can be observed that the variation in MHE performance is lesser for noisy data compared to EKF.

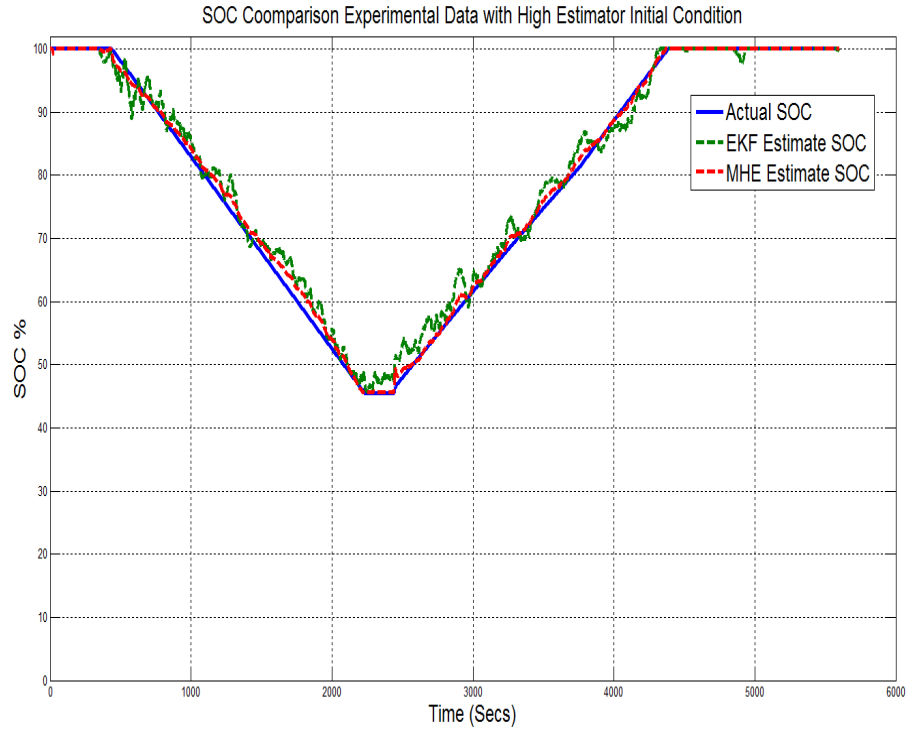


Fig. 5.4. SOC Comparison Experimental Data with High Estimator Initial Condition

5.4 Comparing Root Mean Square Estimation Error

Root mean square errors for the SOC estimations for the transient cycle under nominal conditions with no variabilities added are calculated and shown in Table 5.2. The results shows that the MHE can reduce the RMSE by almost 50 % for estimations even though the initial conditions are not known accurately.

5.5 Comparing Battery SOH Estimation

As stated earlier in this work SOH is considered as a measure of bulk capacitance of the battery which is one of the states of the model developed. Because of the unavailability of the degraded battery data the battery model itself is used to introduce the various levels of degradation. BS Bhangu et al has showed the use

Table 5.2
 Root Mean Square Errors Calculated for Transient Current, SOC Estimation with EKF and MHE

	Est. Init. State < Actual		Est. Init. State = Actual		Est. Init. State > Actual	
	MHE	EKF	MHE	EKF	MHE	EKF
RMSE V_b	0.1778	0.3028	0.0001	0.0002	0.1678	0.2104
RMSE V_{cs}	0.1786	0.3033	0.0004	0.0004	0.1703	0.2130
RMSE V_o	0.1779	0.3034	0.0033	0.0034	0.1623	0.2055
RMSE C_{bulk}	0.0515	1.2252	0.0001	0.001	0.0291	0.4520
SOC	0.03	0.11	0.05	0.09	0.07	0.16

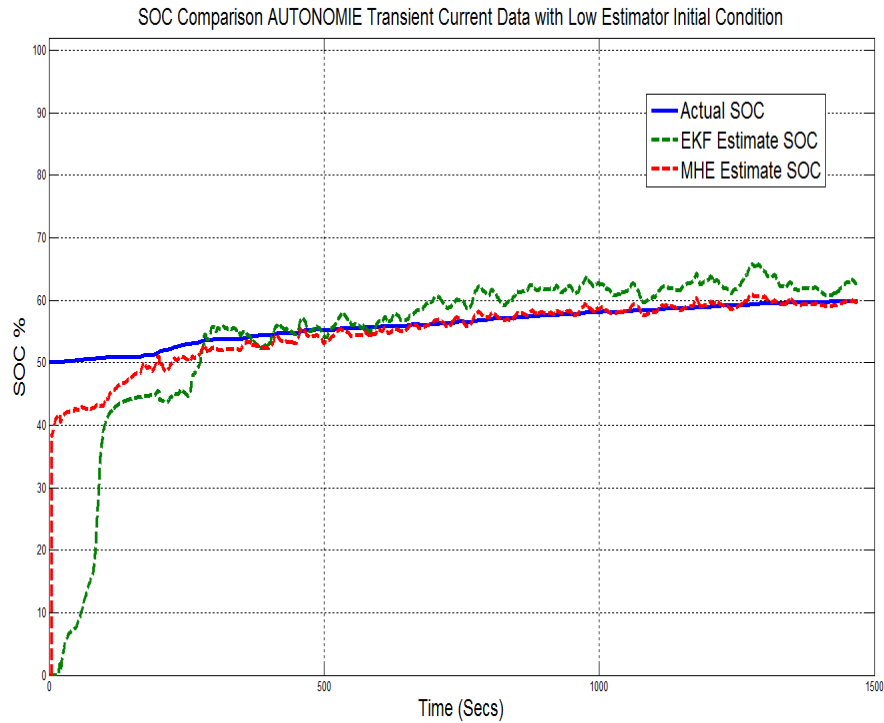


Fig. 5.5. SOC Comparison AUTONOMIE Transient Data with Low Estimator Initial Condition

of Bulk Capacitance based SOH estimation on a similar Equivalent Circuit Battery Model [15]. In their work it is shown that the estimated Bulk Capacitance is reduced up to 60000 Farads from an initial value of around 80000 Farads before the battery stopped to perform a desired cycle. Their SOH estimation strategy took about 50000 Secs to converge to the actual SOH. In this SoH estimation study, the battery model is initialized with different C_{bulk} capacitance values as below and the estimated bulk capacitance from both EKF and MHE are compared in Figure 5.19 and 5.20.

Healthy System 88370.8 Farads Degraded System I 78370.8 Farads Degraded System II 68370.8 Farads Degraded System III 58370.8 Farads

From Figures 5.19 and 5.20 it can be observed that MHE converges to the actual value of bulk capacitance of the battery cell very quickly, whereas EKF is not able to

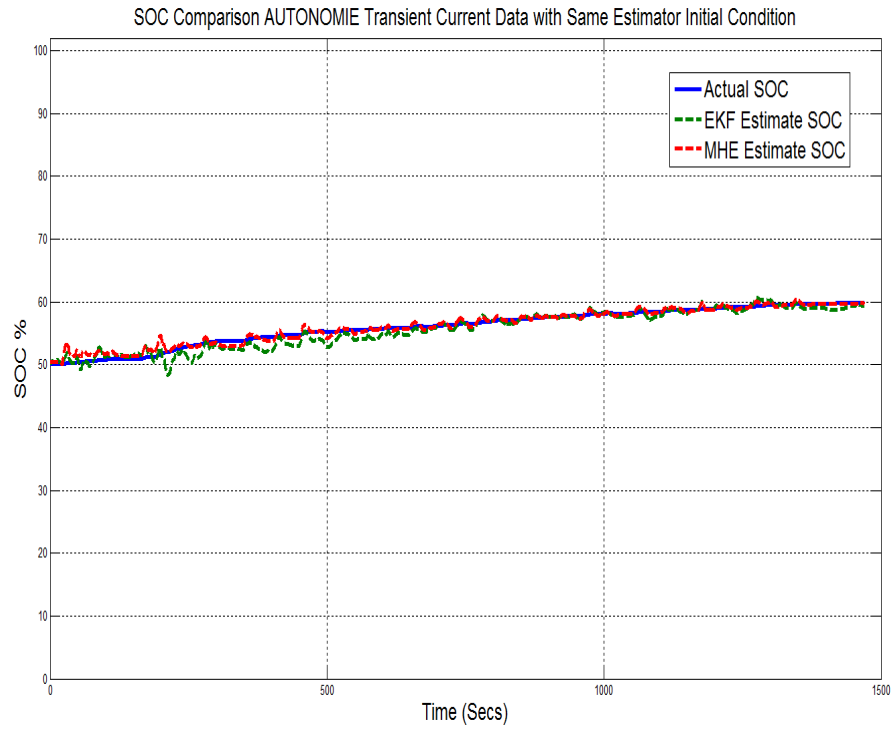


Fig. 5.6. SOC Comparison AUTONOME Transient Data with Same Estimator Initial Condition

converge within the time frame of the simulation. Hence MHE can be employed for accurately predicting the SOH of the battery online.

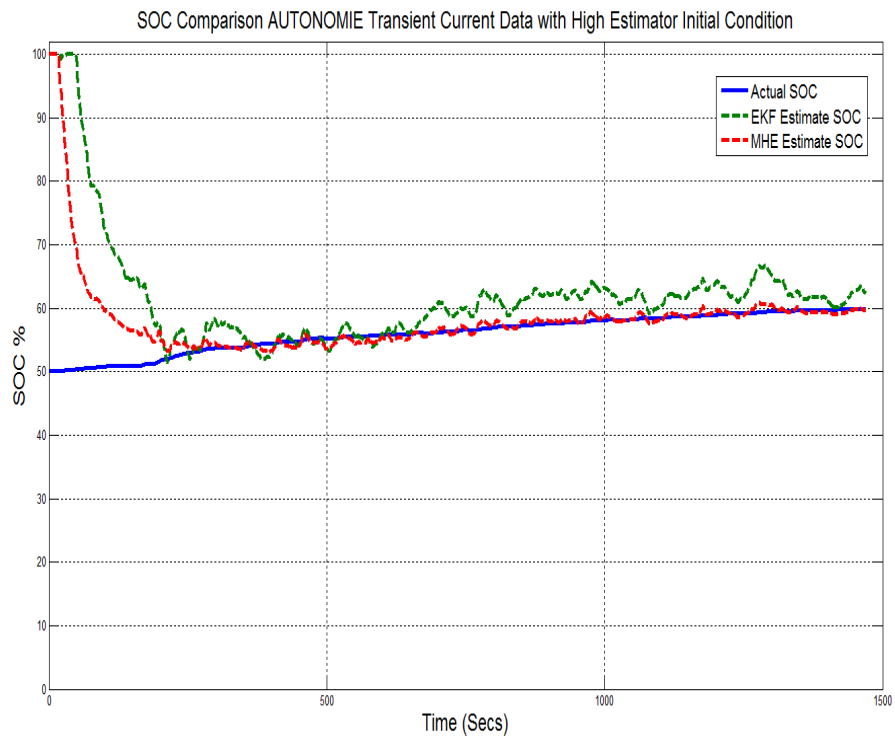


Fig. 5.7. SOC Comparison AUTONOMIE Transient Data with High Estimator Initial Condition

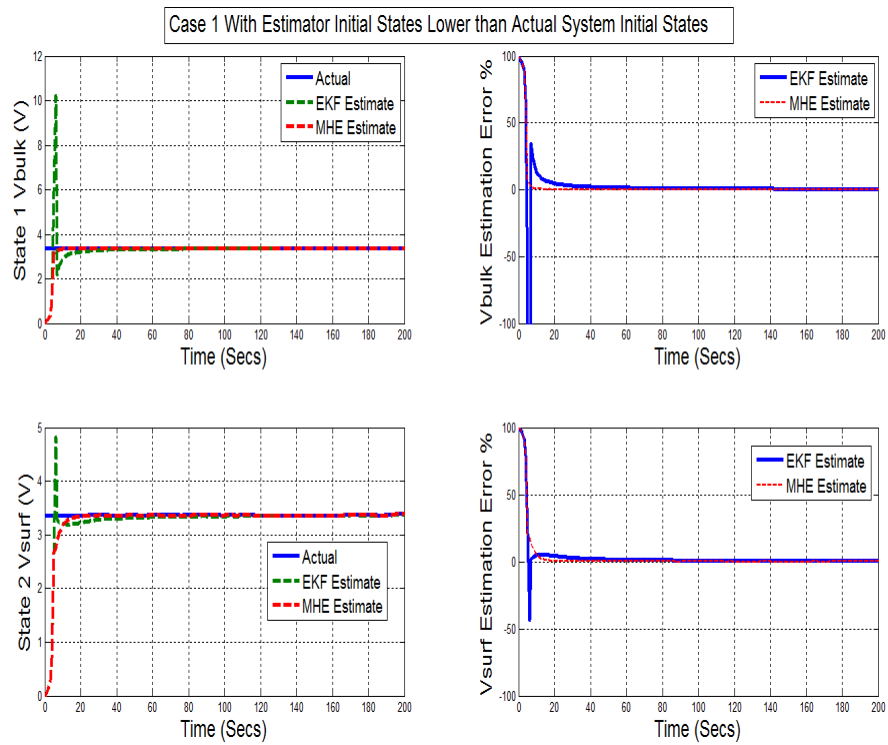


Fig. 5.8. Battery States V_{bulk} and V_{surf} Estimation Compared for Estimator Initial Condition Case I

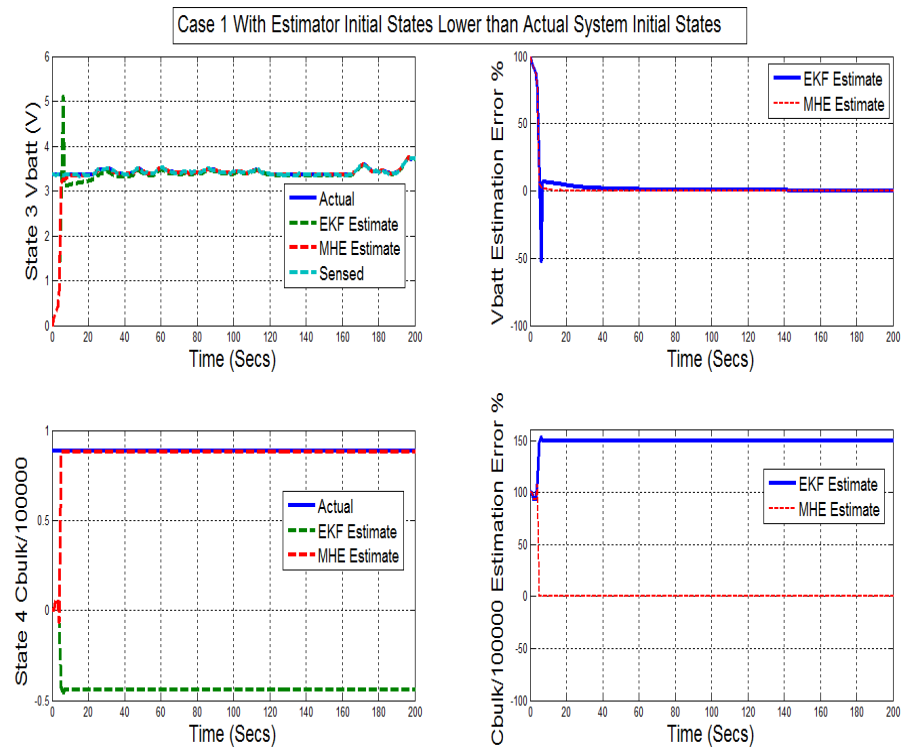


Fig. 5.9. Battery States Vbatt and Cbulk Estimation Compared for Estimator Initial Condition Case I

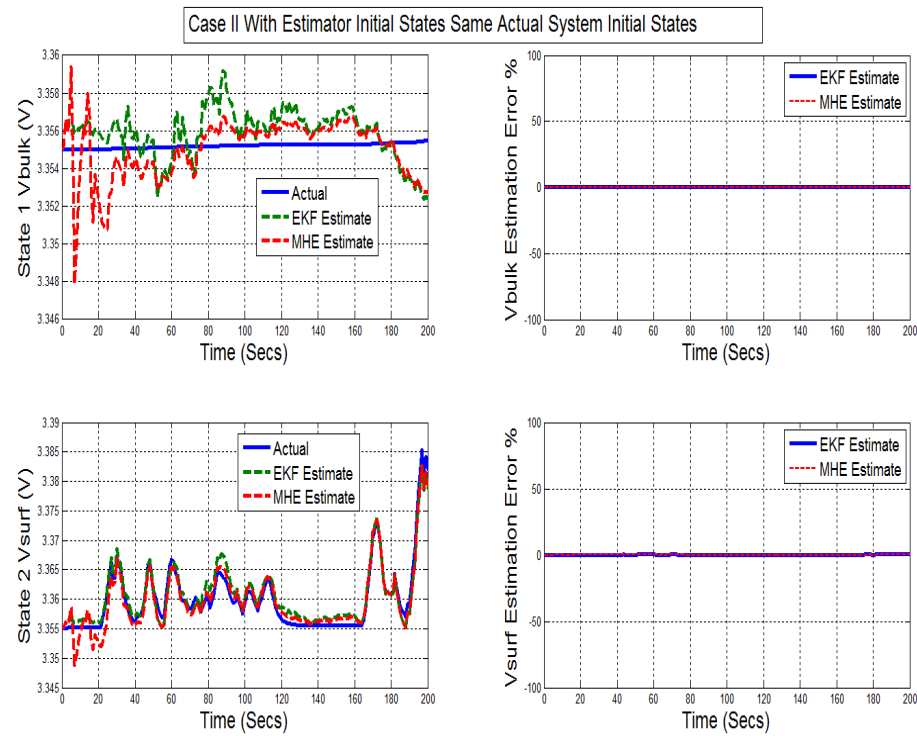


Fig. 5.10. Battery States V_{bulk} and V_{surf} Estimation Compared for Estimator Initial Condition Case II

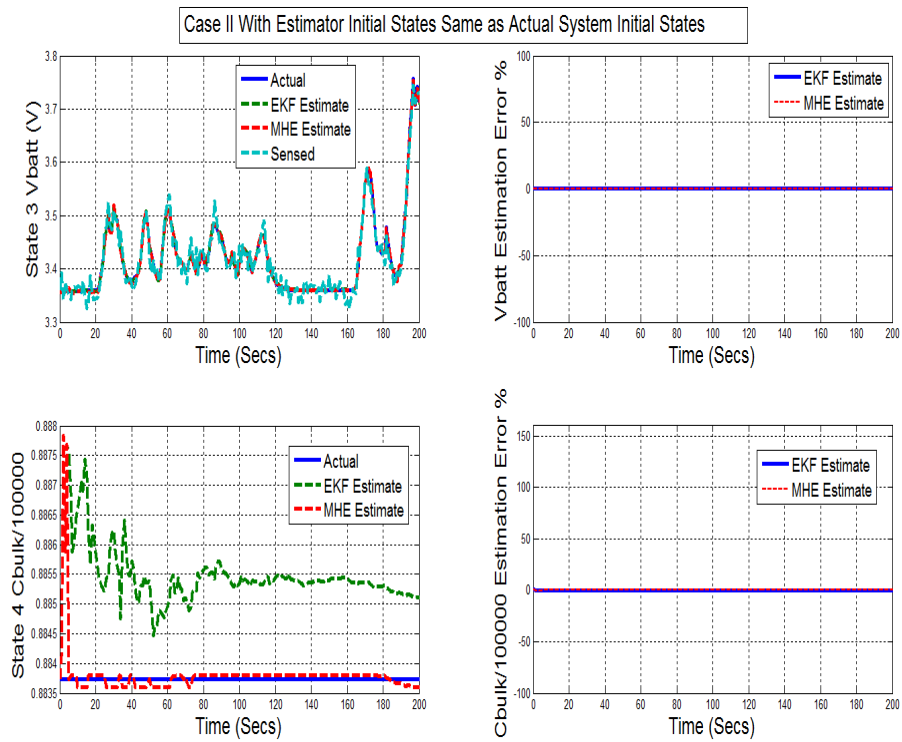


Fig. 5.11. Battery States V_{batt} and C_{bulk} Estimation Compared for Estimator Initial Condition Case II

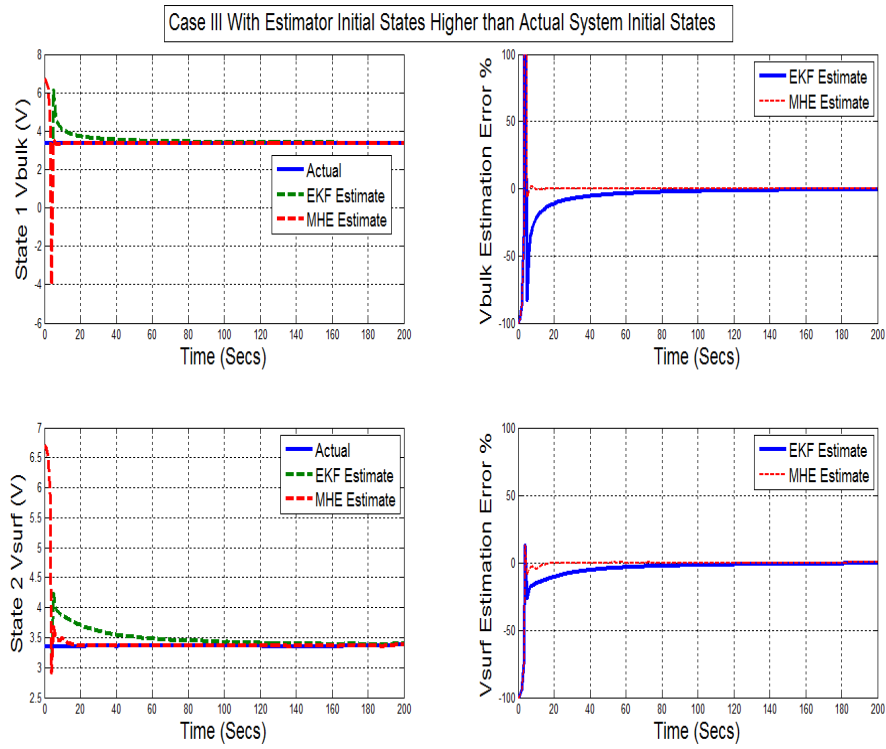


Fig. 5.12. Battery States V_{bulk} and V_{surf} Estimation Compared for Estimator Initial Condition Case III

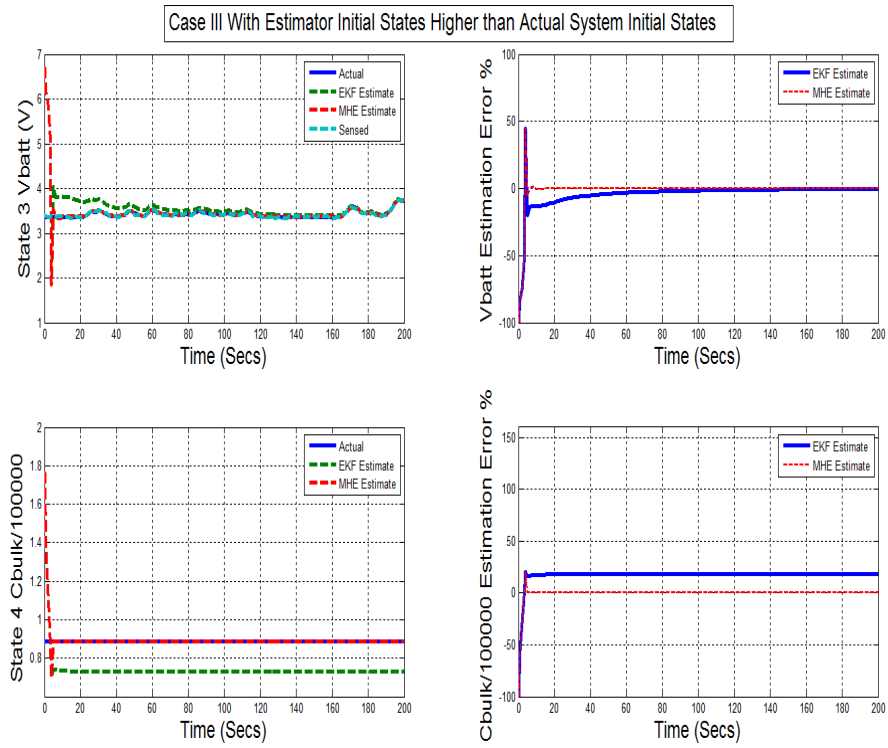


Fig. 5.13. Battery States V_{batt} and C_{bulk} Estimation Compared for Estimator Initial Condition Case III

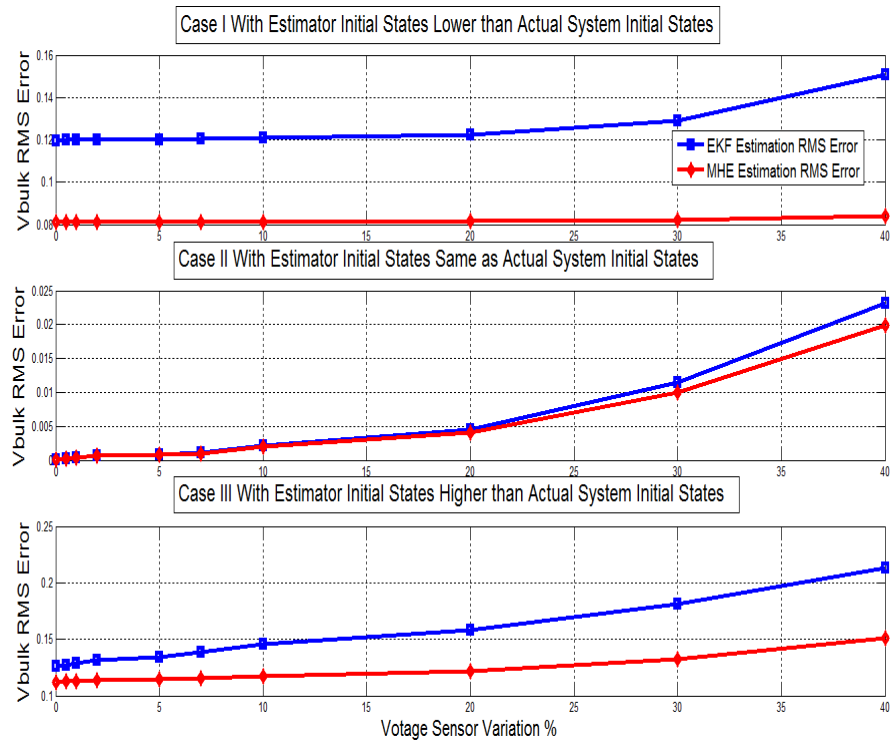


Fig. 5.14. Comparing the RMS Error for State 1 V_{bulk} , between the MHE and EKF estimators with various Voltage Sensor Measurement Noise

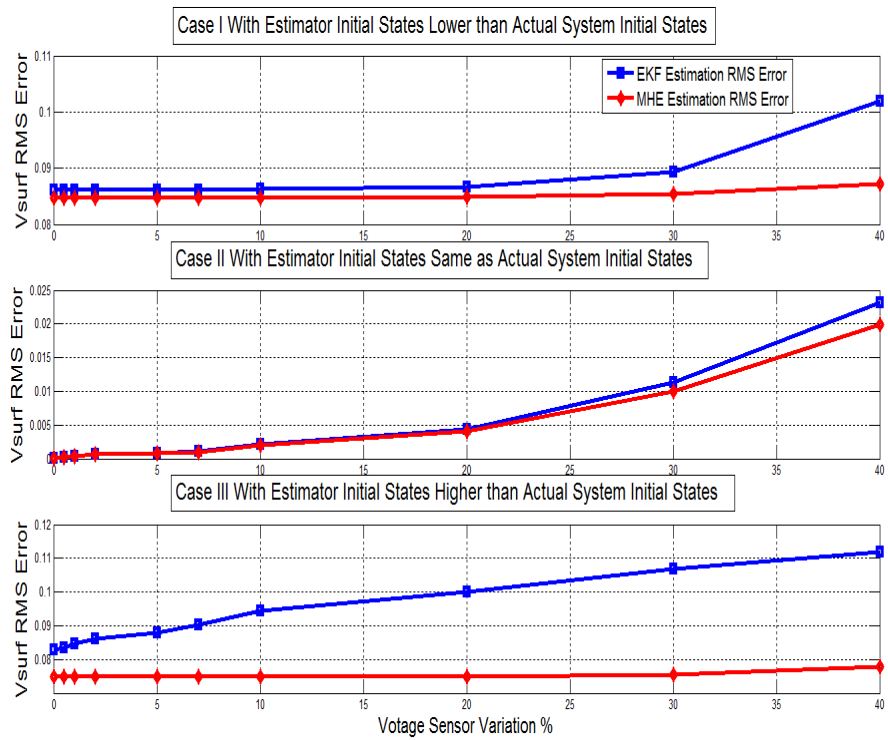


Fig. 5.15. Comparing the RMS Error for State 2 V_{surf} , between the MHE and EKF estimators with various Voltage Sensor Measurement Noise

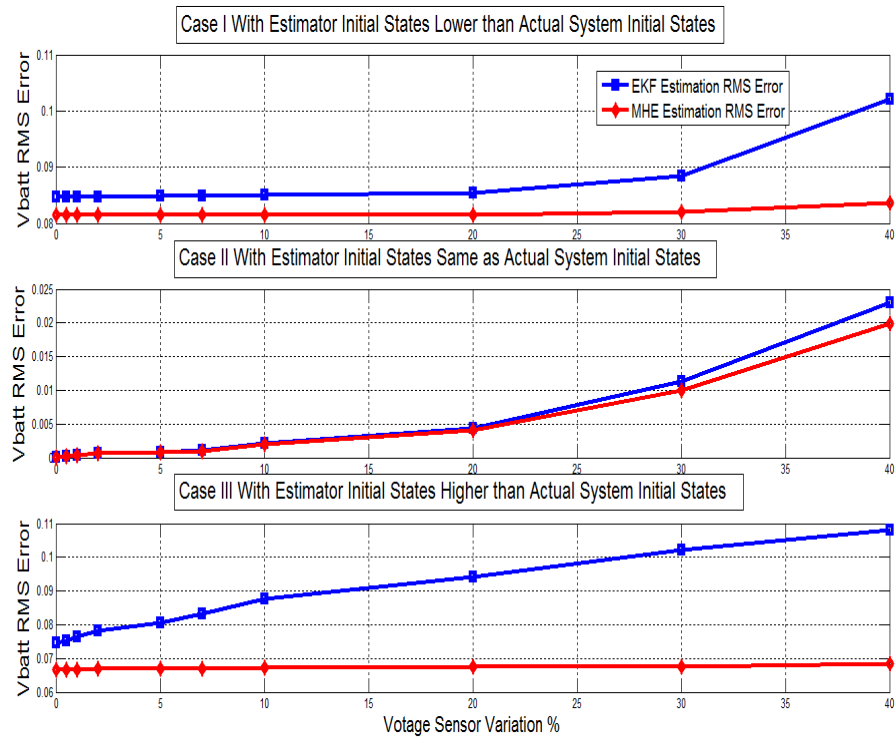


Fig. 5.16. Comparing the RMS Error for State 3 V_{batt} , between the MHE and EKF estimators with various Voltage Sensor Measurement Noise

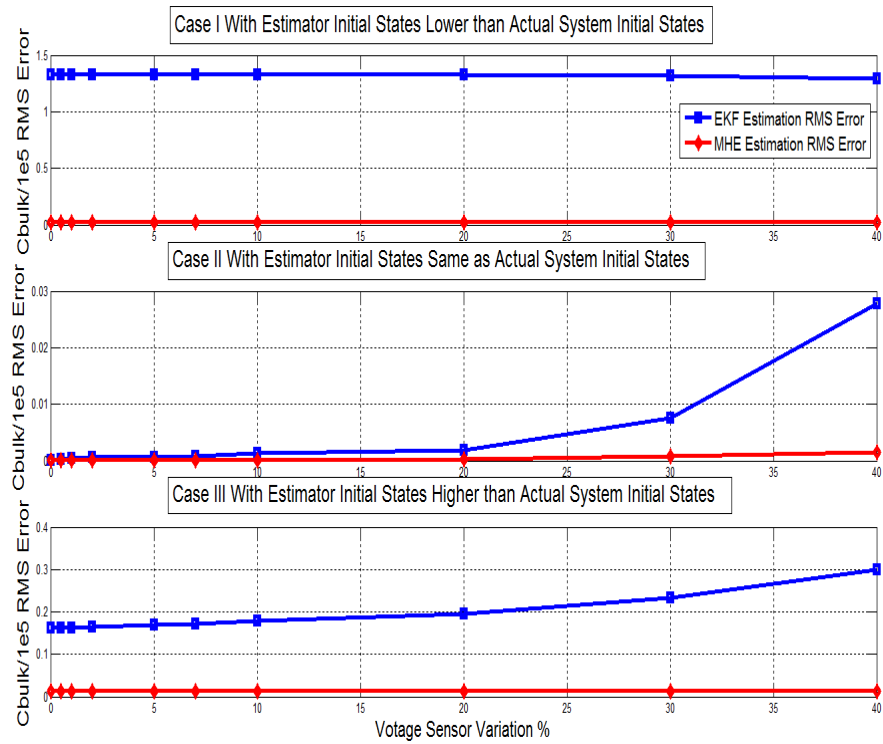


Fig. 5.17. Comparing the RMS Error for State 4 Bulk Capacitance, between the MHE and EKF estimators with various Voltage Sensor Measurement Noise

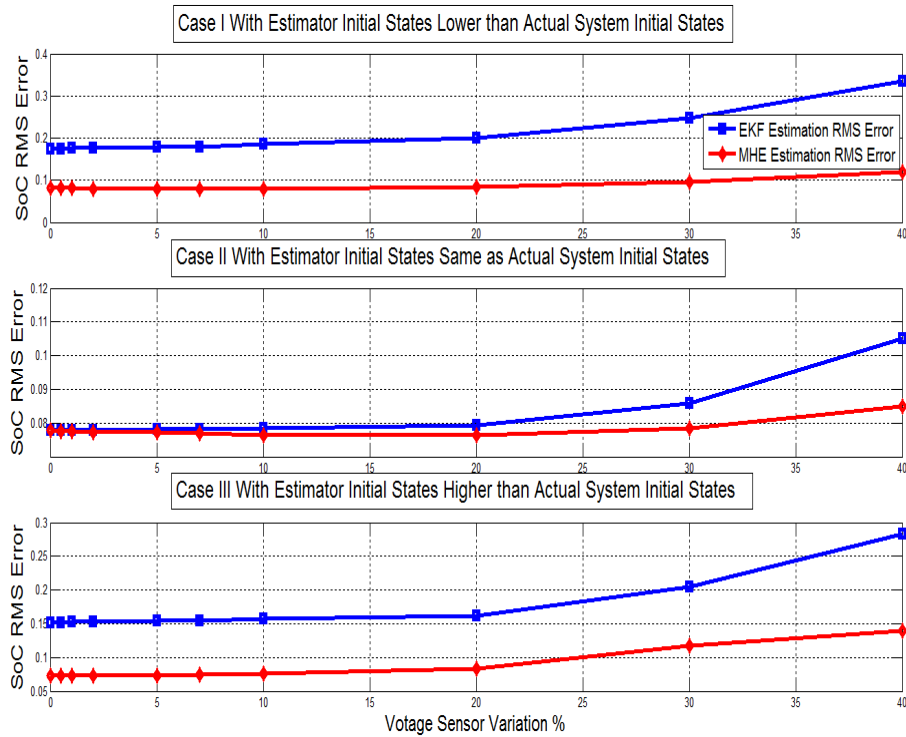


Fig. 5.18. Comparing the RMS Error for Estimated SOC, between the MHE and EKF estimators with various Voltage Sensor Measurement Noise

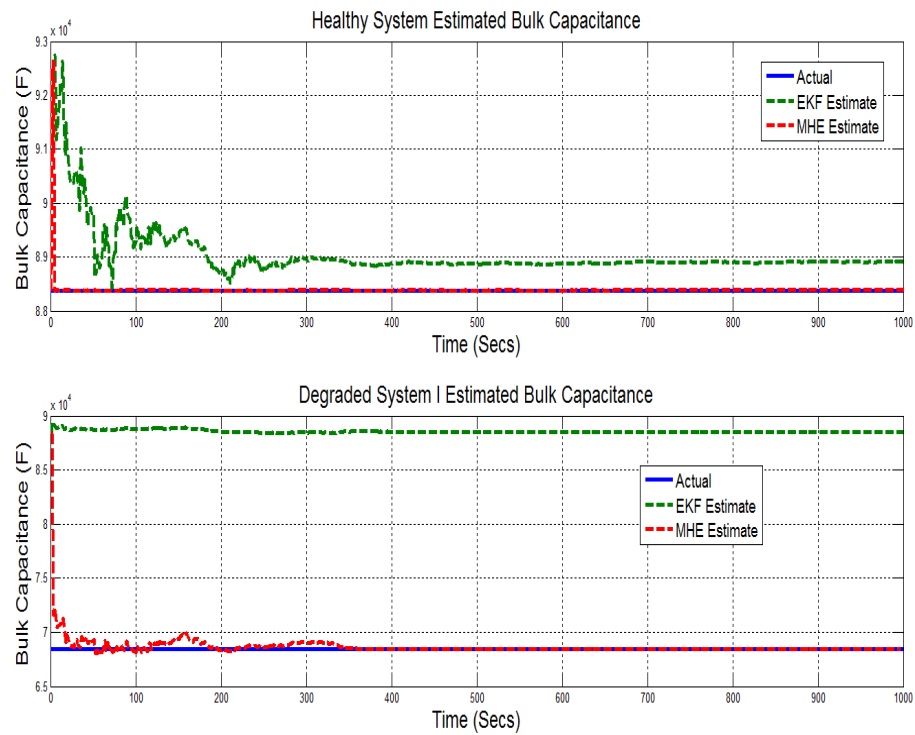


Fig. 5.19. Bulk Capacitance Estimation comparison for SOH Estimation. Healthy and Degraded System I

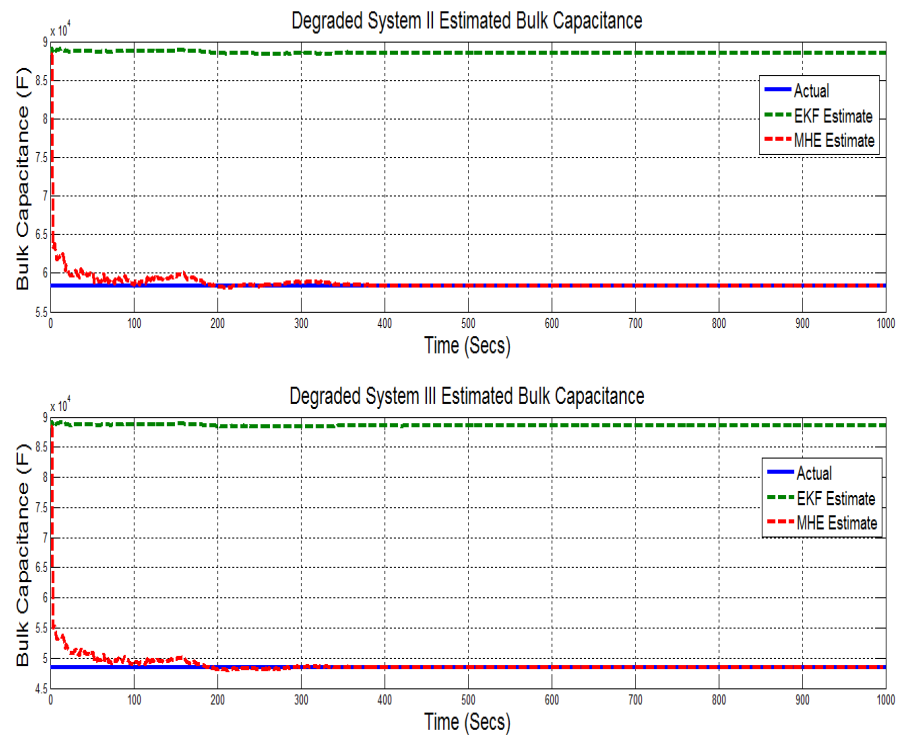


Fig. 5.20. Bulk Capacitance Estimation comparison for SOH Estimation. Healthy and Degraded System II

6. CONCLUSION

6.1 Conclusion

Knowing the state information of a battery system is very important in Battery Management Systems. But most of the critical states such as SOC and SOH are not directly measurable using the existing measurement systems. So state estimators are used in the past to estimate the states. But these estimator's performance vary a lot based on the estimator initial conditions and measurement noises. A moving horizon estimation (MHE) strategy is implemented to estimate the states of a battery and the performance of the estimator is compared against the traditional Kalman filter techniques. The following are the observations made in this work.

- An equivalent circuit battery model is used in the study to model battery dynamics.
- Experimental data is used to tune and validate the model parameters and the validated model is used for state estimation.
- An Extended Kalman Filter and a proposed Moving Horizon Estimation algorithms are developed and implemented using Matlab and Simulink.
- The estimator performances are compared for different initial conditions and measurement noises.
- Results shows that in all cases MHE performed better than EKF. The convergence time of EKF with different initial state guess is found to be about 100 Secs, whereas MHE converged to the actual state within 20 Secs. For the Bulk capacitance state of the model EKF did not converge to the actual stage whereas MHE did. So there is a benefit in employing the MHE for estimating SOH of

the battery real time. EKF might take a long time to show any trend of health degradation.

- MHE is found to be robust to measurement and process noise. A sensor measurement noise of 0 to +/- 40 % normally distributed measurement error is induced into the estimators. Results showed that MHE can perform even under noisy conditions. Even though the estimator error increased with increased sensor noise, the RMSE is significantly less than EKF.
- Estimator performances with different initial conditions are also evaluated. Results shows that estimator errors can be reduced upto 50 % compared to EKF estimator if the initial state of the system is wrong or is unknown.
- Because of the additional computational complexity involved MHE ran about 1.5 to 1.7 times slower compared to EKF on a 64 bit Windows 8 machine.
- The results shows Moving Horizon Estimation can be used as an alternative way for not using the highly accurate but complex to solve electrochemical battery models. A reasonably accurate battery model which captures the basic battery dynamics along with the horizon based estimation can give better estimation results and overcome modelling deficiencies.
- For the next generation of model based robust control design and model based diagnostic technologies Moving Horizon Estimation can be employed on the on-board computers.

6.2 Recommendation for Future Work

In the future, extension of the current work can be performed towards real world validation of the Moving Horizon Estimation for battery state estimation.

- As a next step Moving Horizon Estimation based state estimation can be implemented on an on-board computers and validate the performance online with battery system in the loop.
- Robustness evaluation of the MHE on real world scenarios.
- Extension of the work to use the MHE state estimation for a Model Predictive Control for the Battery Management System.
- Evaluation of MHE on battery data with non-Gaussian, non-zero mean measurement noise distributions.
- Evaluation of different optimization solvers for MHE, which will reduce the computational cost in on-board computers.
- Evaluation of more complex battery models such as electrochemical models with Moving Horizon Estimators.
- Evaluate the potential of faster optimization algorithms to improve the speed of MHE.

LIST OF REFERENCES

LIST OF REFERENCES

- [1] H. Bergveld, W. Kruijt, and P. Notten, "Battery management systems," in *Battery Management Systems*, vol. 1 of *Philips Research*, pp. 9–30, Springer Netherlands, 2002.
- [2] E. Karden, *Using Low Frequency Impedance Spectroscopy for Characterization, Monitoring, and Modeling of Industrial Batteries*. Aachener Beiträge des ISEA, Shaker Verlag, 2002.
- [3] S. Piller, M. Perrin, and A. Jossen, "Methods for state-of-charge determination and their applications," *Journal of power sources*, vol. 96, no. 1, pp. 113–120, 2001.
- [4] K. Kutluay, Y. Cadirci, Y. S. Ozkazanc, and I. Cadirci, "A new online state-of-charge estimation and monitoring system for sealed lead-acid batteries in telecommunication power supplies," *Industrial Electronics, IEEE Transactions on*, vol. 52, no. 5, pp. 1315–1327, 2005.
- [5] O. Caumont, P. Le Moigne, C. Rombaut, X. Muneret, and P. Lenain, "Energy gauge for lead-acid batteries in electric vehicles," *Energy Conversion, IEEE Transactions on*, vol. 15, no. 3, pp. 354–360, 2000.
- [6] T. Torikai, T. Takesue, Y. Toyota, and K. Nakano, "Research and development of model-based battery state of charge indicator," in *Industrial Electronics, Control, Instrumentation, and Automation, 1992. Power Electronics and Motion Control., Proceedings of the 1992 International Conference on*, pp. 996–1001, IEEE, 1992.
- [7] F. Huet, R. Nogueira, L. Torcheux, and P. Lailler, "Simultaneous real-time measurements of potential and high-frequency resistance of a lab cell," *Journal of power sources*, vol. 113, no. 2, pp. 414–421, 2003.
- [8] H. Blanke, O. Bohlen, S. Buller, R. W. De Doncker, B. Fricke, A. Hammouche, D. Linzen, M. Thele, and D. U. Sauer, "Impedance measurements on lead-acid batteries for state-of-charge, state-of-health and cranking capability prognosis in electric and hybrid electric vehicles," *Journal of power Sources*, vol. 144, no. 2, pp. 418–425, 2005.
- [9] A. Hammouche, E. Karden, and R. W. De Doncker, "Monitoring state-of-charge of ni-mh and ni-cd batteries using impedance spectroscopy," *Journal of Power Sources*, vol. 127, no. 1, pp. 105–111, 2004.
- [10] M. Hughes, R. Barton, S. Karunathilaka, N. Hampson, and R. Leek, "The residual capacity estimation of fully sealed 25 a h lead/acid cells," *Journal of power sources*, vol. 17, no. 4, pp. 305–329, 1986.

- [11] F. Huet, "A review of impedance measurements for determination of the state-of-charge or state-of-health of secondary batteries," *Journal of power sources*, vol. 70, no. 1, pp. 59–69, 1998.
- [12] G. L. Plett, "Extended kalman filtering for battery management systems of lipb-based hev battery packs: Part 1. background," *Journal of Power sources*, vol. 134, no. 2, pp. 252–261, 2004.
- [13] G. L. Plett, "Extended kalman filtering for battery management systems of lipb-based hev battery packs: Part 2. modeling and identification," *Journal of power sources*, vol. 134, no. 2, pp. 262–276, 2004.
- [14] G. L. Plett, "Extended kalman filtering for battery management systems of lipb-based hev battery packs: Part 3. state and parameter estimation," *Journal of power sources*, vol. 134, no. 2, pp. 277–292, 2004.
- [15] B. S. Bhangu, P. Bentley, D. A. Stone, and C. M. Bingham, "Nonlinear observers for predicting state-of-charge and state-of-health of lead-acid batteries for hybrid-electric vehicles," *Vehicular Technology, IEEE Transactions on*, vol. 54, no. 3, pp. 783–794, 2005.
- [16] J. Han, D. Kim, and M. Sunwoo, "State-of-charge estimation of lead-acid batteries using an adaptive extended kalman filter," *Journal of Power Sources*, vol. 188, no. 2, pp. 606–612, 2009.
- [17] S. Lee, J. Kim, J. Lee, and B. Cho, "State-of-charge and capacity estimation of lithium-ion battery using a new open-circuit voltage versus state-of-charge," *Journal of power sources*, vol. 185, no. 2, pp. 1367–1373, 2008.
- [18] J. Lee, O. Nam, and B. Cho, "Li-ion battery soc estimation method based on the reduced order extended kalman filtering," *Journal of Power Sources*, vol. 174, no. 1, pp. 9–15, 2007.
- [19] D.-T. Lee, S.-J. Shiah, C.-M. Lee, and Y.-C. Wang, "State-of-charge estimation for electric scooters by using learning mechanisms," *Vehicular Technology, IEEE Transactions on*, vol. 56, no. 2, pp. 544–556, 2007.
- [20] C.-C. Hua, T.-Y. Tasi, C.-W. Chuang, and W.-B. Shr, "Design and implementation of a residual capacity estimator for lead-acid batteries," in *Industrial Electronics and Applications, 2007. ICIEA 2007. 2nd IEEE Conference on*, pp. 2018–2023, IEEE, 2007.
- [21] S. Drouilhet, B. L. Johnson, *et al.*, "A battery life prediction method for hybrid power applications," in *AIAA Aerospace Sciences Meeting and Exhibit*, 1997.
- [22] K. Takeno, M. Ichimura, K. Takano, and J. Yamaki, "Influence of cycle capacity deterioration and storage capacity deterioration on li-ion batteries used in mobile phones," *Journal of power sources*, vol. 142, no. 1, pp. 298–305, 2005.
- [23] M.-S. Wu and P.-C. J. Chiang, "High-rate capability of lithium-ion batteries after storing at elevated temperature," *Electrochimica acta*, vol. 52, no. 11, pp. 3719–3725, 2007.

- [24] R. Jaworski, "Effects of nonlinearity of arrhenius equation on predictions of time to failure for batteries exposed to fluctuating temperatures," in *Telecommunications Energy Conference, 1998. INTELEC. Twentieth International*, pp. 289–296, 1998.
- [25] U. Tröltzsch, O. Kanoun, and H.-R. Tränkler, "Characterizing aging effects of lithium ion batteries by impedance spectroscopy," *Electrochimica Acta*, vol. 51, no. 8, pp. 1664–1672, 2006.
- [26] M. Broussely, S. Herreyre, P. Biensan, P. Kasztejna, K. Nechev, and R. Staniewicz, "Aging mechanism in li ion cells and calendar life predictions," *Journal of Power Sources*, vol. 97, pp. 13–21, 2001.
- [27] M. Wohlfahrt-Mehrens, C. Vogler, and J. Garche, "Aging mechanisms of lithium cathode materials," *Journal of power sources*, vol. 127, no. 1, pp. 58–64, 2004.
- [28] T. Osaka, S. Nakade, M. Rajamäki, and T. Momma, "Influence of capacity fading on commercial lithium-ion battery impedance," *Journal of power sources*, vol. 119, pp. 929–933, 2003.
- [29] D. U. Sauer and H. Wenzl, "Comparison of different approaches for lifetime prediction of electrochemical systems using lead-acid batteries as example," *Journal of Power Sources*, vol. 176, no. 2, pp. 534–546, 2008.
- [30] B. Suthar, V. Ramadesigan, P. Northrop, B. Gopaluni, S. Santhanagopalan, R. Braatz, and V. Subramanian, "Optimal control and state estimation of lithium-ion batteries using reformulated models," in *American Control Conference (ACC), 2013*, pp. 5350–5355, June 2013.
- [31] V. Johnson, "Battery performance models in advisor," *Journal of power sources*, vol. 110, no. 2, pp. 321–329, 2002.
- [32] "Autonomie vehicle simulation software. last accessed in dec 2014. <http://www.autonomie.net/>."
- [33] G. Welch and G. Bishop, "An introduction to the kalman filter," 1995.
- [34] K. Reif, S. Günther, E. YAZ SR, and R. Unbehauen, "Stochastic stability of the discrete-time extended kalman filter," *IEEE Transactions on Automatic Control*, vol. 44, no. 4, pp. 714–728, 1999.
- [35] D. G. Robertson, J. H. Lee, and J. B. Rawlings, "A moving horizon-based approach for least-squares estimation," *AIChE Journal*, vol. 42, no. 8, pp. 2209–2224, 1996.
- [36] M. A. Grover and R. Xiong, "A modified moving horizon estimator for in situ sensing of a chemical vapor deposition process," *Control Systems Technology, IEEE Transactions on*, vol. 17, no. 5, pp. 1228–1235, 2009.
- [37] "Flatness approach to fault parametric detection of systems. last accessed in dec 2014. <http://article.sapub.org/10.5923.j.eee.20120202.09.html> ."
- [38] D. G. Robertson and J. H. Lee, "On the use of constraints in least squares estimation and control," *Automatica*, vol. 38, no. 7, pp. 1113–1123, 2002.

- [39] C. V. Rao, *Moving horizon strategies for the constrained monitoring and control of nonlinear discrete-time systems*. PhD thesis, University of Wisconsin-Madison, 2000.